Climate change key driver of extreme drought in water scarce Sicily and Sardinia

Authors

1. Mariam Zachariah, *Grantham Institute - Climate Change and the Environment, Imperial College London, UK*
2. Guido Fioravanti, *European Commission, Joint Research Centre, Ispra, Italy*
3. Juan Camilo Acosta Navarro, *European Commission, Joint Research Centre, Ispra, Italy*
4. Joyce Kimutai, *Grantham Institute - Climate Change and the Environment, Imperial College London, UK*
5. Alessandro Dosio, *European Commission, Joint Research Centre, Ispra, Italy*
6. Luigi Pasotti, *Servizio Informativo Agrometeorologico Siciliano (SIAS) - Sicilia Orientale*
7. Maja Vahlberg, *Red Cross Red Crescent Climate Centre, The Hague, the Netherlands (based in Ubmeje/Umeå, Sweden)*
8. Carolina Pereira Marghidan, *Red Cross Red Crescent Climate Centre, the Hague, Netherlands, KNMI, De Bilt, Netherlands; University of Twente, Enschede, Netherlands*
9. Friederike Otto, *Grantham Institute - Climate Change and the Environment, Imperial College London, UK*

Review authors

10. Ben Clarke, *Grantham Institute - Climate Change and the Environment, Imperial College London, UK*
11. Sjoukje Philip, *Royal Netherlands Meteorological Institute (KNMI), De Bilt, The Netherlands*
12. Elena Nalato, *Italian Red Cross, Rome, Italy*
13. Lorenzo Stefano Massucchielli, *Italian Red Cross, Rome, Italy*
14. Bruna Taccardi, *Italian Red Cross, Rome, Italy*
15. Roop Singh, *Red Cross Red Crescent Climate Centre, the Hague, the Netherlands (based in New Jersey, USA)*

Main findings

- The main economic activities in Sicily, agriculture and tourism, both strongly depend on water availability. The economic consequences of this drought are thus catastrophic for many in the region and recovery will take time. In Sardinia, agriculture is economically less important, but of high cultural relevance; leading to challenges with water prioritisation for domestic and agricultural use on both islands.
- Natural ecosystems also suffer. Agricultural expansion, especially in Sicily, has increased water demand, with a decrease of 62ha per year since 1990 in natural ecosystems, including wetlands.
- In different observational datasets the extreme drought, defined by SPEI12 (fig. 1) is among the most severe droughts since records began. All data agree that this drought is not very rare in Sardinia in today's climate that has warmed by 1.3°C primarily due to the burning of fossil fuels, with a return period of about 10 years (3 - 93 years). In Sicily, such a drought does not occur very often, with a best estimated return period of around 100 years (10- 200,000 years) in today's climate.
- Based on the US Drought Monitoring Classification system, the 1-in-10 year drought over Sardinia which is an 'extreme' (D3) drought now would be classified as a 'severe' (D2) drought without the effects of climate change, and with further warming would be a more severe 'extreme' drought (D3). The rare 1-in-100 year drought over Sicily which is also an 'extreme' (D3) drought would be a 'severe' (D2) drought without climate change, and with a further 0.7C of warming, will become an 'exceptional' drought (D4).
- To understand the meteorological drivers of these changes in drought, we also assess the individual components making up the drought index, namely rainfall, potential evapotranspiration and temperature. We find that changes in rainfall are small and not statistically significant: on the contrary, both values observed for potential evapotranspiration and temperature as observed this year would have been almost impossible to occur without human-induced climate change. We thus conclude that this increase in drought severity is primarily driven by the very strong increase in extreme temperatures due to human-induced climate change.
- It has been well-established that climate models tend to underestimate the increase in extreme temperatures in Europe; this in part accounts for the discrepancy between the observed change in drought frequency and intensity and those represented in climate models.
- Unless the world rapidly stops burning fossil fuels, these events will become even more common in the future. In a world 2°C warmer than preindustrial, which could happen as soon as 2050 without large and rapid reductions in greenhouse gas emissions, droughts like the ones in Sicily and Sardinia will become more frequent.
- Effective drought risk management in regions such as Sardinia and Sicily requires a sustained focus on long-term preparedness and adaptation. Investing in resilient infrastructure, water conservation strategies, and sustainable resource management is crucial to mitigating the impacts of drought.

1 Introduction

Sicily and Sardinia, the two largest Italian islands and important centres of agriculture and tourism, have suffered from exceptionally low rainfall and very high temperatures over the last 12 months, culminating in extreme drought conditions from May 2024 onwards.

Following an autumn with much below average rain, 2024 was warm and dry in Southern Italy for most of the year, with drought alerts being issued as early as December in Sicily and from May onwards in Sardinia. After sectoral acts for livestock and drinkwater in some provinces in February and March, in May 2024 Sicily declared a state of emergency. The drought is still ongoing, and, with the end of the boreal summer approaching, water reservoirs on the two islands are almost empty, despite water rationing having been in place since February. With severe rationing, water has not been available for irrigation in many significant areas, with severe consequences for agriculture and livestock.

The severe drought over the islands of Sicily and Sardinia since the summer of 2023 is part of a widespread event that has been affecting large parts of the Mediterranean region driven and characterised by a persistent lack of precipitation and temperatures well above the normal (Toreti et al, 2024c). In Sicily, the second half of 2023 marked an unprecedented dry spell, being the most arid period in over a century. From September to December, the total deficit of rainfall reached approximately 220 millimetres. Notably, the final month of the year recorded staggering precipitation shortfalls of up to 96% in certain areas, particularly impacting the provinces of Enna, which averaged a deficit of -81.5%, and Catania, which saw an average reduction of -80%. While the regional annual balance does not reflect such a dire situation (approximately 160 millimeters shy of the average), it is essential to highlight that this is primarily due to the extreme weather events that struck the island during the first half of the year (Source: Sicilian Agrometeorological Information Service). These events included the "medicane" in early February over Eastern Sicily, which brought about remarkable rainfall totals of up to 310 mm in just 48 hours. Additionally, other significant weather occurrences in May and June yielded similar accumulations over just two days, while the overall regional average for 2023 remains below 600 millimeters. These conditions have been causing damaging impacts on agricultural systems in several locations, further exacerbating the impacts from droughts in the previous two years (Toreti et al., 2023). The drought has been especially extreme in southern and southeastern Europe, crippling availability of water resources. This year, the coastal regions of the Mediterranean islands began feeling the impacts as early as January, with the persistent lack of precipitation and warmer-than-average temperatures leading to severe negative soil moisture anomalies and poor vegetation conditions (Toreti et al., 2024a). These conditions have been persisting well into mid 2024, extending the drought conditions in both Sicily and Sardinia.

According to the European Commission Joint Research Centre (JRC) Combined Drought Indicator (CDI) for drought early warning and agricultural drought monitoring, the twelve months from August 2023 to July 2024 has been very dry over both Sicily and Sardinia (Fig. 1.1). The CDI combines information from the spatial patterns of anomalous precipitation, soil moisture and greenness of vegetation to categorise drought severity based on increasing intensity as: ‘watch’, ‘warning’ and ‘alert’. It should be noted that ‘alert’ levels can only be achieved in areas with an active crop cycle, when precipitation, soil moisture as well as greenness of vegetation all show signs of drought. Since

September 2023, both islands have been almost completely under drought conditions- at ‘warning’ or ‘alert’ levels, implying that during this period, at least precipitation deficits and low soil moisture conditions were widespread, with vegetation also affected in some months of active crop cycles, especially in Sicily.

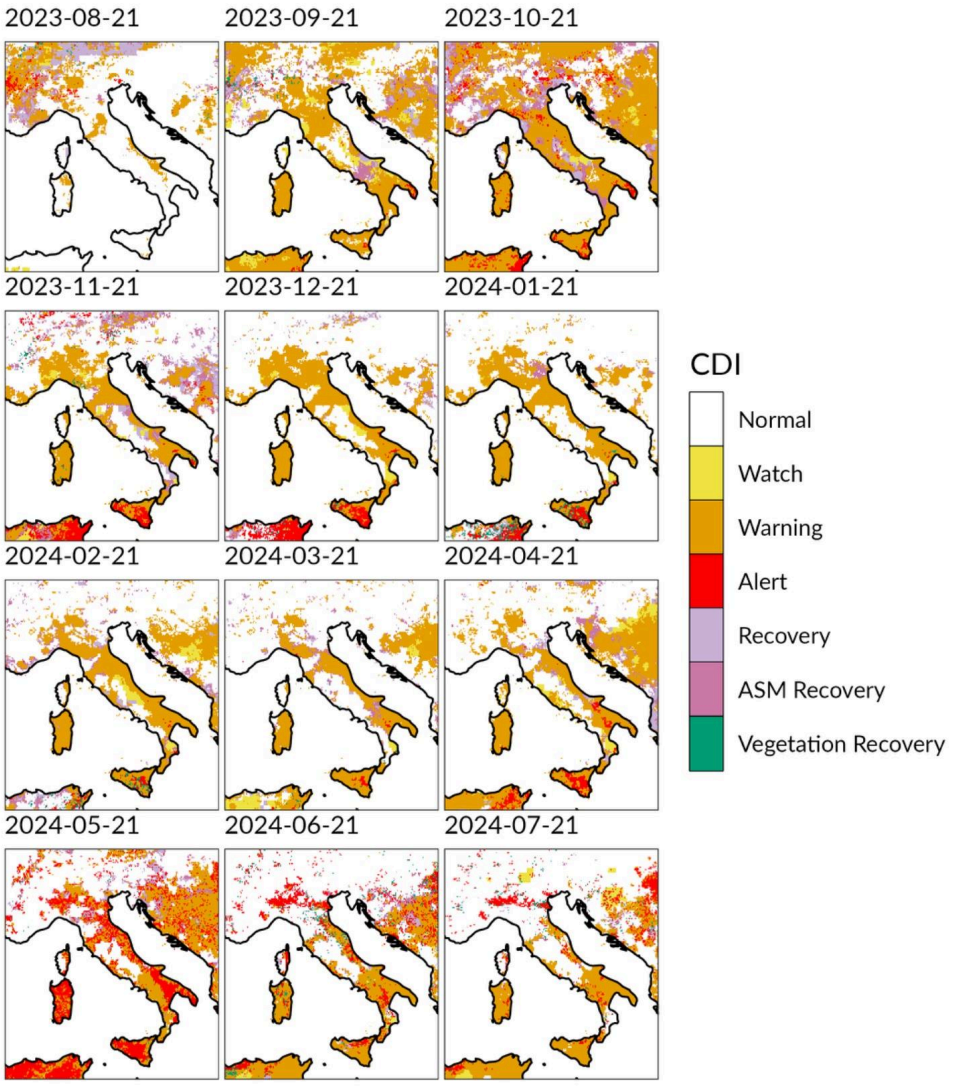

Figure. 1.1. Combined Drought Indicator (CDI) over Italy for the last dekad (21st -end of month) of each month for the 12 months from Aug 2023 to July 2024 [Source: Copernicus European Drought Observatory, European Commission JRC].

Fig. 1.2 shows the monthly mean time series of area-averaged precipitation, temperature, standardised soil moisture anomalies (SMA) and Fraction of the Photosynthetically Active Radiation (FAPAR), which is a measure of vegetation greenness, for the islands of Sicily and Sardinia. The precipitation over both islands have been below normal for most part of the year- more extreme over Sicily as compared to Sardinia. The lower than normal precipitation was accompanied by high temperatures- highest in the last 30 years in Sicily for most part of the year and over Sardinia for the first part of the year (till February 2024) and continued to be high afterwards. Concurrent hot and dry conditions can exacerbate soil moisture deficits and vegetation health. Monthly mean time series of area-averaged standardised SMA (middle panels-Fig. 1.2) show exceptional drought conditions in both islands since

September 2023, with lowest values since 1995 in the respective months. The parchedness (or lack of greenness) of vegetation (bottom panels in Fig. 1.2) is pronounced over Sicily during this period as indicated by the negative FAPAR values implying that the vegetation had been parched since autumn, with a brief recovery during January-February and intensifying again the following spring through summer of 2024. Over Sardinia, the signs of unhealthy vegetation are limited to the summer months of 2024, likely a lagged response of vegetation to the water deficit signals in the other variables. During the period from September 2023 to July 2024, FAPAR anomalies in Sicily were the lowest since 2012 during many months, but that is not the case in Sardinia.

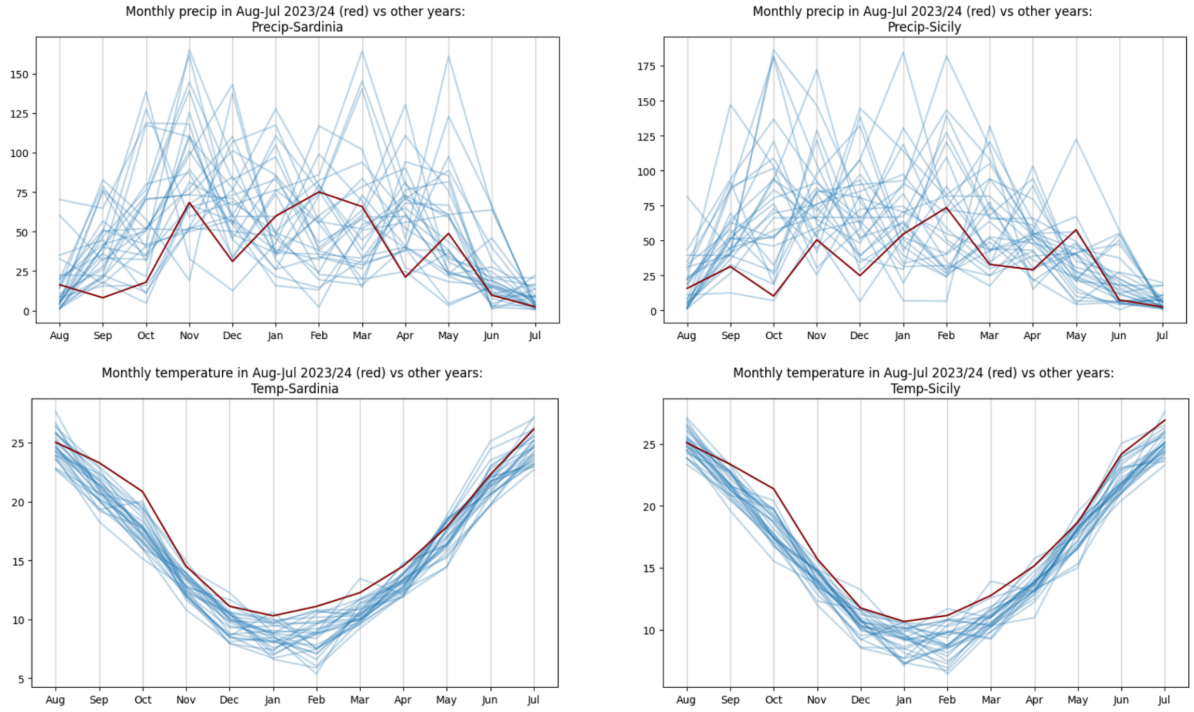

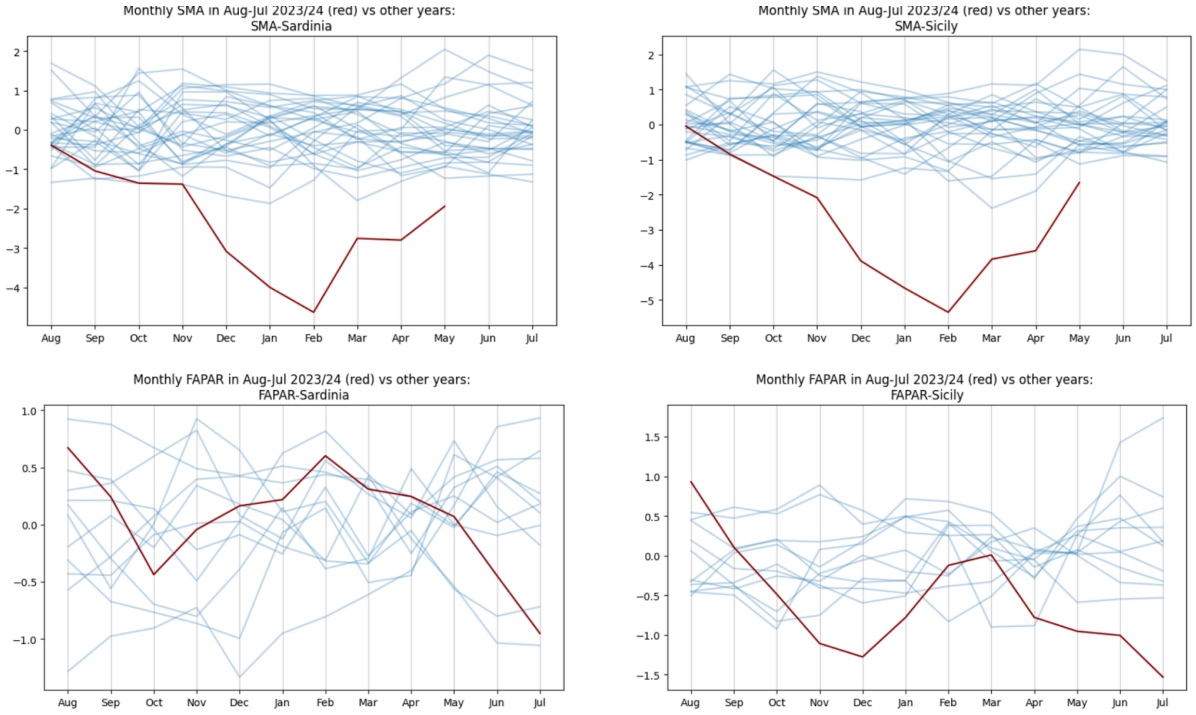

Figure. 1.2. (top) Monthly precipitation over Sardinia (top left) and Sicily (top right) during all years (running from Aug-July, blue lines) since 1995 (2012 for FAPAR anomaly). The red line shows the values during Aug2023-July2024. (upper middle) same as the top panel, for temperature. (lower middle) same as the top panel, for Soil Moisture Anomaly (SMA). (bottom) same as the top panel, for Fraction of the Photosynthetically Active Radiation (FAPAR) anomaly.

From the discussions above, it emerges that although precipitation was below normal, the extremity of the drought was likely intensified by accompanying high temperatures, as seen in the extreme soil moisture anomalies (SMA) and significant reductions in vegetation greenness (FAPAR). This highlights how elevated temperatures contributed to worsening the drought's impact on the soil and vegetation, despite the precipitation deficit. Therefore, for defining this event, we use the Standardised Precipitation Evapotranspiration Index (SPEI) the 12 month period from August 2023 to July 2024. This index accounts for changes in not only precipitation, but also potential evapotranspiration (PET), which is a key determinant of water availability for both ecosystems and agricultural activity, and thereby providing a comprehensive measure of the drought severity. Figure 1.3 shows the SPEI-12 during Aug-2023-July 2024 over a slightly big region around Italy (2.5˚E-21.25˚E 35˚N-47.5˚N), and the classification of the drought severity during this period, following the US Drought Monitor classification system (normal (SPEI $\geq$ 0.49), D0 - abnormally dry (-0.79 $\leq$ SPEI $\leq$ -0.5), D1 - moderate (-1.29 $\leq$ SPEI $\leq$ -0.8) , D2 - severe (-1.59 $\leq$ SPEI $\leq$ -1.3), D3 - extreme (-1.99 $\leq$ SPEI $\leq$ -1.6), and D4 - exceptional (SPEI $\leq$ -2)).

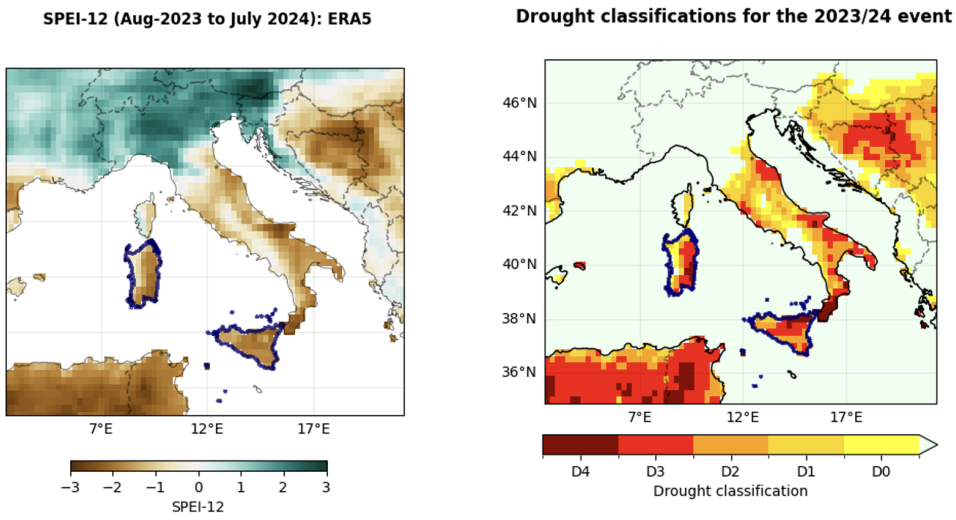

Figure 1.3. (left) The 12-month SPEI in July, 2024 over Italy. (right) Drought classification of the event categorised according to the US Global Drought Monitor system. The study regions- the islands of Sicily and Sardinia are outlined in dark blue.

Precipitation trends in Europe show a general increase in the north and a decrease in the south, particularly in winter, though trends in southern Europe vary significantly depending on the time period examined (Fischer and Knutti, 2016; Knutson and Zeng, 2018; Atlas.8). From 1980 to 2015, annual mean precipitation trends are generally positive in northern, eastern, and western Europe, with significant spatial variability, while in the Mediterranean, trends are less consistent and only significant in specific areas (Lionello et al., 2012; MedECC, 2020).

Drought assessments for Southern Europe, including the region of interest in Chapters 11, 12 and 8 of the IPCC WG1 report. Southern Europe is one of the regions for which there is high confidence in observed changes as well as the projected increase in the frequency and severity of droughts. This trend is attributed to rising temperatures- a key contributor for exacerbating drought conditions by increasing evapotranspiration and reducing soil moisture, and changing precipitation patterns caused by climate change. The confidence in them is based on multiple lines of evidence, including observational data, climate models, and physical understanding of the processes driving these changes. Chapter 11 also notes a projected decrease in precipitation, particularly during the summer. This projected reduction in rainfall will likely contribute to more frequent and severe drought conditions. The chapter also highlights that the likelihood of compound events, where droughts coincide with heatwaves have increased considerably and are projected to increase further with increases in global warming levels.

Droughts in Southern Europe pose significant risks to agriculture, particularly rain-fed crops like cereals, olives, and grapes. Reduced water availability for irrigation could further exacerbate these risks. Prolonged droughts can lead to forest dieback, loss of biodiversity, and increased susceptibility to wildfires, which are already a growing concern in the region. According to the European Drought Risk Atlas (Rossi et al., 2023), drought impact estimates for agriculture under current climate conditions show that reductions in crop yield may be substantial. Average annual reductions in yield are estimated as up to 10% less than the expected amounts, with the highest risks located in the

Mediterranean area. The IPCC in its Synthesis Report underscores the potential for droughts to exacerbate water scarcity, leading to conflicts over water resources, economic losses, and increased migration pressures. As for water supplies, the effects of droughts on public water supply are difficult to simulate. Nevertheless, under projected climate conditions, drought-induced water abstraction is expected to increase around the Mediterranean, especially at global warming levels of +2 °C, and +3 °C (Rossi et al., 2023).

2 Data and methods

2.1 Observational data

Several datasets were used for extracting precipitation, maximum and minimum temperature to describe droughts . These datasets are described in detail below. All three variables were extracted at daily frequency starting from the beginning of the respective records to July 31,2024.

1. The ERA5 reanalysis product (Hersbach et al., 2020) from European Centre for Medium-Range Weather Forecasts (ECMWF), which is available from 1950 at 0.25° × 0.25° spatial resolution. It should be noted that the variables from ERA5 are not directly assimilated, but these are generated by atmospheric components of the Integrated Forecast System (IFS) modelling system. In addition to the precipitation, maximum and minimum temperatures, estimates of potential evaporation is also available in this dataset. Potential evaporation in the IFS is based on surface energy balance calculations with the vegetation parameters set to 'crops/mixed farming' and assuming 'no stress from soil moisture' (see here). These estimates are also used to get an independent estimate of SPEI, for evaluating the fidelity of the empirical estimates of PET based on temperature in capturing drought features over the region.

2. The Climate Prediction Centre (CPC) gridded product from NOAA Physical Sciences Laboratory (PSL) known as the CPC Global Unified Daily Gridded data are constructed from a network of rain gauges, weather stations and satellites (Xie et al., 2010; CPC FTP pages) , is available at 0.5° x 0.5° resolution, for the period 1979-present. Data are available from NOAA.

3. The Multi-Source Weighted-Ensemble Precipitation (MSWEP) v2.8 dataset (updated from Beck et al., 2019) is another global gridded dataset, available at daily time steps and at 0.1° spatial resolution, available from 1979 to near real-time. This product combines gauge-, satellite-, and reanalysis-based data.

Observations of daily rainfall from a large network of stations over the islands of Sicily and Sardinia were used for evaluating the gridded datasets for their aptness in capturing the trends and year-to-year variability. The climatological values for Sicily and Sardinia (Piervitali et al.,2022) have been retrieved from the national system for climate data collection, processing and dissemination called Sistema Nazionale per l'Elaborazione e Diffusione di Dati Climatici (SCIA), developed by the Italian Institute for Environmental Protection and Research (ISPRA), in collaboration with the main institutions which operate meteorological networks in Italy. (Desiato et al., 2011). SCIA collects more than 9000 daily time series of temperature and precipitation from several meteorological,

agrometeorological and hydrographic networks across the 20 Italian regions. Within SCIA, the daily records undergo quality controls, with regular updates annually (Fioravanti et al., 2019). The data can be explored at the page https://valori-climatici-normali.isprambiente.it.

Figure 2.1 shows the area-averaged annual accumulated rainfall over Sicily and Sardinia, comparing each of the gridded datasets with the station averages. Over both regions ERA5 is found to closely align with the station-based estimates in terms of magnitude, variability and trends. The other two datasets- MSWEP and CPC are found to do reasonably well in their representation of the variability and the trends over both regions, but CPC is found to systematically underestimate the magnitudes, likely due to the coarser resolution of this dataset as compared to the others..

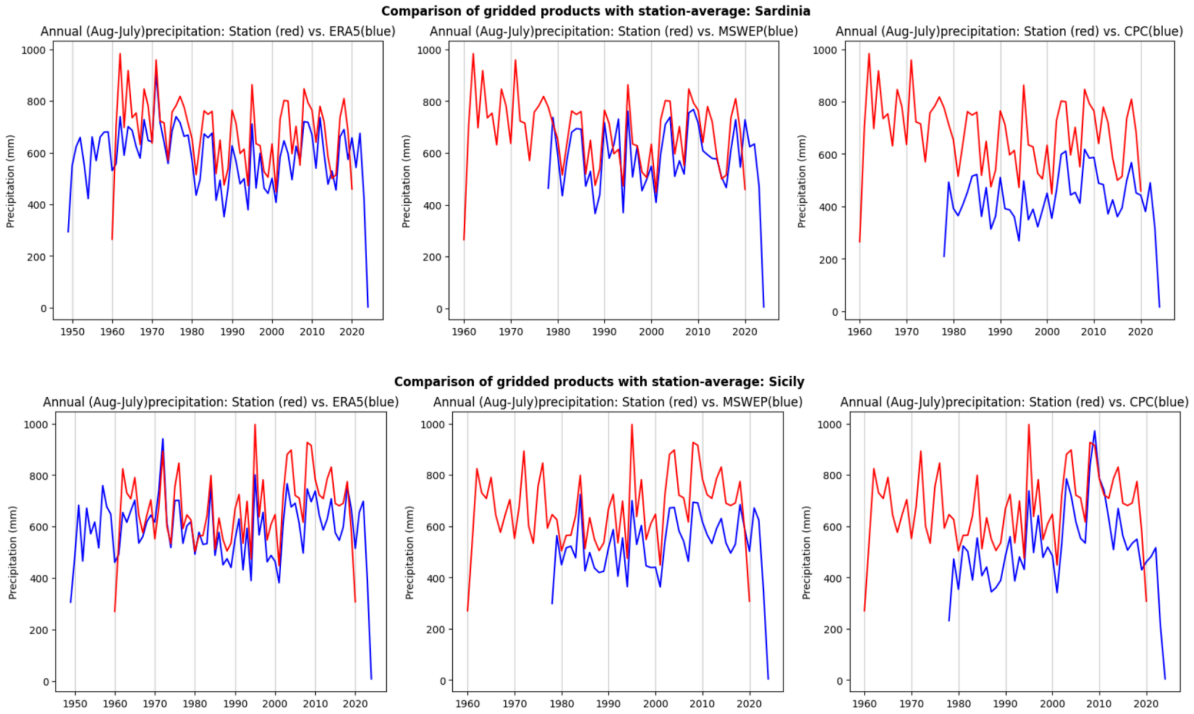

Figure 2.1. (top) Comparison of the area-averages from the selected gridded datasets - ERA5 (top-left), MSWEP (top middle) and CPC (top right) vs. station-averaged estimates, for Sardinia. (bottom) same as (top) for Sicily.

In addition to the datasets described above, the CDI dataset was also used in this study. The CDI served as a qualitative metric to both understand the progression of drought since the summer of 2023 (see Fig. 1.1) and to evaluate the effectiveness of the selected drought metric- the Standardised Precipitation Evapotranspiration Index (SPEI)- in tracking the event over this period. This dataset, a collection of raster maps generated by the Copernicus European Drought Observatory (EDO; https://drought.emergency.copernicus.eu/), is used for monitoring agricultural drought in Europe. The CDI blends information from three key indicators: the Standardised Precipitation Index (SPI), the Soil Moisture Anomaly (SMA) and the Fraction of the Photosynthetically Active Radiation (FAPAR) anomaly. These are complemented by the use of monthly varying snow and crop masks to exclude areas covered with snow or without an active crop cycle, respectively. The CDI 10-daily maps have been downloaded from EDO. The CDI dataset has a spatial resolution of 1/24 decimal degrees (around 5 km), a temporal resolution of 10 days and is available from 2012 onward.

Soil moisture is a critical component for agricultural drought monitoring, as crop growth conditions largely depend on the water stored in the soil (Wu et al., 2021). The SMA, which has been

downloaded from the Copernicus European Drought Observatory (EDO) as GeoTIFF 10-daily maps, is derived from model-based daily estimates of the Soil Moisture Index (SMI), is derived from the top two soil layers of the JRC hydrological model LISFLOOD (Burek et al., 2013). This dataset is available from 1995 onward, at 1/24 decimal degrees (~5km) and at 10-day intervals. Similarly, the FAPAR anomaly, another component of the CDI, is the fraction of the Photosynthetically Active Radiation (a ratio that ranges from 0 to 1 with no units) that is actually absorbed by vegetation. FAPAR is commonly employed as an indicator of the greenness state of vegetation (photosynthetic activity, Gobron et al., 2005). The FAPAR anomaly, also available as GeoTIFF 10-daily maps from EDO, has a spatial resolution of 1/24 decimal degrees (around 5km), a temporal resolution of 10 days and is available from 2012 onward. In EDO, the FAPAR anomaly indicator is computed using the global VNP15A2H product from VIIRS (Myneni, 2023), freely available through the Land Processes Distributed Active Archive Center (LP DAAC).

Finally, as a measure of anthropogenic climate change for the attribution analysis, we use the (low-pass filtered) global mean surface temperature (GMST) taken from the National Aeronautics and Space Administration (NASA) Goddard Institute for Space Science (GISS) surface temperature analysis (GISTEMP, Hansen et al., 2010 and Lenssen et al. 2019).

2.2 Model and experiment descriptions

We use a multi-model ensemble of regional climate models (RCMs) from the Coordinated Regional Climate Downscaling Experiment (CORDEX)- European Domain (EURO-CORDEX) at 0.11 degree resolution (EUR-11) (Jacob et al., 2014; Vautard et al., 2021). The ensemble consists of 65 runs from pairings of 23 regional climate models driven by 8 GCMs (although the RCM-GCM matrix is incomplete, meaning that not all RCMs downscaled all GCMs), with historical simulations from 1970-2005, and projections up to the year 2100 for different representative concentration pathway (RCP, van Vuuren et al., 2011) RCP8.5. In this study, the first ensemble members from 32 RCM-GCM pairs that were available for download at the time of the analysis were evaluated for their fidelity in modelling precipitation features in the region. 11 RCMs in this set, which were driven by IPSL's IPSL-CM5A-MR and NOAA-GFDL's GFDL-ESM2G GCMs were discarded immediately due to their inability to capture the seasonal cycle of rainfall in Sicily and Sardinia. The remaining 21 models were evaluated for other criteria- namely spatial patterns and the variable distribution (discussed in detail in Section 4).

2.3 Statistical methods

In this analysis we analyse time series from precipitation, temperature and SPEI from ERA5, CPC and MSWEP/MSWX gridded observational datasets . Methods for observational and model analysis and for model evaluation and synthesis follow the World Weather Attribution Protocol, described in Philip et al. (2020), with supporting details found in van Oldenborgh et al. (2021), Ciavarella et al. (2021) and here.

The analysis steps include: (i) trend calculation from observations; (ii) model validation; (iii) multi-method multi-model attribution and (iv) synthesis of the attribution statement.

We calculate the return periods, Probability Ratio (PR; the factor-change in the event's probability) and change in intensity of the event under study in order to compare the climate of now and the climate of the past, defined respectively by the (smoothed) GMST values of now and of the preindustrial past (1850-1900, based on the Global Warming Index), where the difference of the smoothed GMST between now and past is 1.3C. To statistically model the event under study, we use the Gaussian distribution that scales (for precipitation) and/or shifts (for temperature and SPEI) with GMST. Next, results from observations and models that pass the validation tests are synthesised into a single attribution statement.

3 Observational analysis: return period and trend

3.1 Analysis of gridded data

3.1.1 SPEI

Fig. 3.1(a) shows the results from fitting non-stationary Gaussian distributions to the annual time series of SPEI-12 (Aug-July) area-averaged over Sardinia from ERA5, MSWEP and CPC datasets. All datasets consistently show a decrease in SPEI values as GMST increases (top panels in Fig. 3.1(a)), suggesting that the droughts are becoming more severe due to global warming. In today's climate which has warmed by 1.3C since pre-industrial era, the 2024 drought event has a return period of 10 years (5-37 years) in the ERA5 dataset (bottom left panel in Fig. 3.1(a)). In the other datasets included in the analysis- ERA5 based on pre-calculated potential evaporation (see Section 2.1 for details), MSWEP and CPC- the event has return periods of 12 (6-56), 6 (3-17) and 15 (6-93) years respectively (bottom panel Fig. 3.1(a)). For the attribution analysis, we use a round value of 1-in-10 years defining the drought event over Sardinia.

The decreasing trends in the datasets further suggest that climate change has increased the likelihood and severity of the event, with probability ratios (PRs) of 50 (5.9 - 1100), 160 (16 - 7300), 7.1 (0.39 - 760) and 56 (0.88 - 21000) and more severity increases of 1.4 (0.68 - 2.1), 1.6 (0.89 - 2.4), 0.84 (-0.42 - 2) and -1.4 (-0.044 - 2.6) in ERA5, ERA5-precalc, MSWEP and CPC datasets, respectively. Following the US Drought Monitor Classifications, the 2023/24 drought is categorised as severe, extreme and exceptional in the ERA5, ERA5-precal and CPC datasets respectively, and as a moderate drought in MSWEP. The respective changes in intensity suggests that in all of these datasets, without climate change, SPEI values of similar rarity in the pre-industrial climate would be considered 'normal' in today's climate in the ERA5, ERA5-precal and MSWEP datasets, and abnormally dry in the CPC dataset.

Fig. 3.1(b) shows similar plots for Sicily. In today's climate, the observed drought event has return periods of 64 (17 -672), 43 (13 - 310), 480 (40 - 200000) and 85 (20-2300) years in the ERA5, ERA5-precal, MSWEP and CPC datasets, respectively. Due to the wide range in the best estimated return periods from the datasets, we use a rounded estimate of 100 years to define the event for the attribution analysis. The trends in the datasets are mixed (top panels in Fig. 3.1(b))- with the longer datasets showing a decreasing trend in SPEI while the shorter datasets show no change to increasing trends- however, in the absence of longer station-based datasets, we cannot ascertain the reasons for

this mixed signal, but can only postulate that this could be an artefact of differences arising from the number of stations available, their quality and the contribution from satellites since the 1980s. In ERA5 and the ERA5-precal datasets, climate change is found to increase the chances of a droughts such as this one by about 3.7 times (0.31-49), 13 times (1.2 - 240) in the ERA5 and ERA5-precal datasets, show a decrease in the likelihood with PR of 0.062 (6.6-e05 - 5.3) in MSWEP and no change with PR of 0.77 (0.01 - 42) in the CPC dataset. The respective intensity changes suggest that climate change increased the drought severity by 0.4 units (0.032 - 1.1) and 0.78 units (0.053 - 1.5) in ERA5 and ERA5-precal, decreased by 0.86 units (21 units decrease - 0.53 units increase). As the the distributions for the 2023 and 1.3C climate are close to each other for CPC (bottom right panel in Fig. 3.1 (b)), the best-estimated intensity increase is only 0.092 units (1.5 decrease to 1.1 increase). This means that without climate change, droughts of similar rarity in the pre-industrial climate as the observed event in today's climate, would be milder and categorised as severe, moderate, moderate and extreme in ERA5, ERA5-precal, MSWEP and CPC datasets.

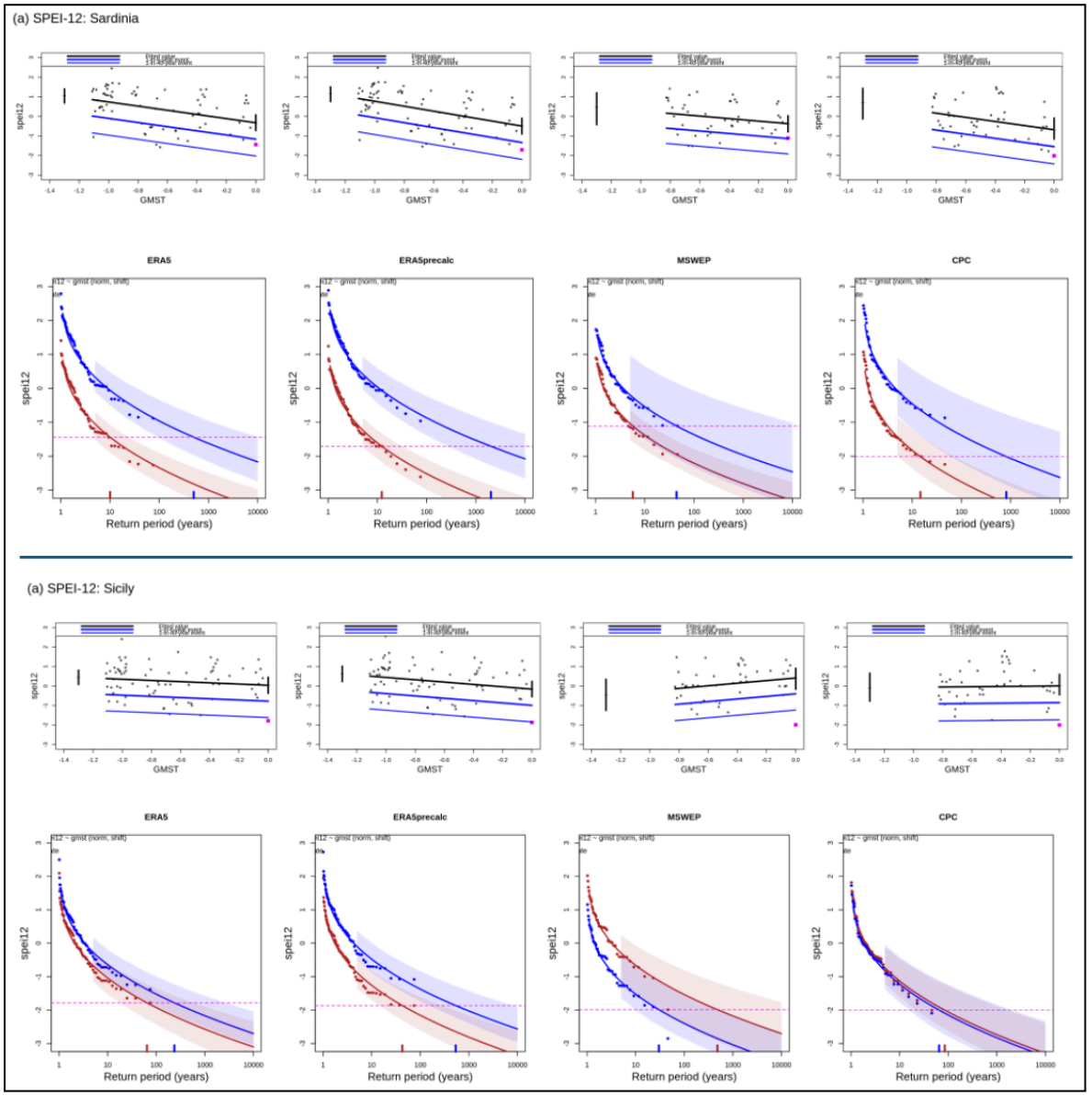

Figure 3.1. (a) Annual SPEI calculated over Sardinia, from ERA5 (left), MSWEP/MSWX (middle) and CPC (right) . (top) The thick red line denotes the time-varying mean, and the thin lines show 1 standard deviation (s.d) and 2 s.d below. The vertical red lines show the 95% confidence interval for the location parameter, for the current 2023 climate and the hypothetical 1.2ºC cooler climate. The 12-month SPEI calculated in July 2024 is given by the magenta box. (bottom) Gaussian return periods of 12-month SPEI for the 2024 climate (red lines) and the 1.3ºC cooler climate (blue lines with 95% CI), calculated using the Hargreaves method from temperatures and precipitation in the respective datasets. (b) same as (a) for Sicily.

3.1.2 Precipitation

While the trends in the drought metric is helpful to understand how droughts will behave under climate change, analysing trends in the main contributing climate variables- namely precipitation and temperature- can help highlight the underlying drivers of the drought patterns. Changes in precipitation can directly influence the frequency, duration and severity of droughts while temperature increases can exacerbate drought conditions by enhancing evaporation rates and reducing soil moisture.

Fig. 3.2 shows the results from fitting non-stationary Gaussian distributions to the annual (Aug-July) precipitation area-averaged over the Sardinia study region based on ERA5, MSWEP and CPC datasets. The low precipitation that Sardinia received during 2023/24 (magenta dots in top panel Fig. 3.2(a)) was not very rare with the region having recorded lower values in the past. The trend in precipitation with respect to increase in global temperature is not consistent across the three datasets- with ERA5 suggesting a decrease in precipitation with global warming, MSWEP registering no trend and CPC showing increasing trend. The event has return periods of 11 (5.4 - 33), 7.2 (3.9 -18) and 18 (8.8 -70) years in the three datasets. A round estimated return period of 10 years is chosen for defining the Sardinia event for the attribution analysis. The Probability Ratios are 3.1 (1.1 - 12), 1 (0.22 - 8) and 0.39 (0.054 - 1.9) in the three datasets, with intensity changes of 13% decrease (1- 24% decrease) , almost no change (22% decrease- 26% increase) and 14% increase (7.9% decrease - 51% increase) in the ERA5, MSWEP and CPC datasets (Fig. 3.2(a, bottom panels)).

The precipitation received in Sicily during the same period was however very low, and the lowest in the CPC and MSWEP records (Fig. 3.2 (b) top panels). Consequently, the return period is very high in the shorter datasets estimated at 89 years (24 - 1400) and 150 years (45 - 3100) in MSWEP and CPC, respectively, reflecting the extremeness of the low precipitation this year. In ERA5, the return period is smaller at 38 years (1.5 - 170 years). The Sicily event is therefore defined as a 1-in-50 year event for the attribution analysis. The near-absence of a trend in rainfall in response to global warming in the ERA5 dataset and the consistent demonstration of increasing trends in the shorter datasets, as shown in Fig. 3.2 (b, top panels), and also noted in ERA5 since 1979 (not shown) suggests that there is likely an increase in annual precipitation received over Sicily during the last 45 years, and the precipitation received this year was unusually low over Sicily. The Probability Ratios are 1 (0.27 - 3.1), 0.14 (0.0071 - 1.2) and 0.2 (0.024 - 1) in the ERA4, MSWEP and CPC datasets, with intensity changes of 0.035% increase (13% decrease - 15% increase), 26% increase (1.8% decrease - 56% increase) and 49% increase (0.14 - 120% increase), respectively (Fig. 3.2(b, bottom panels)).

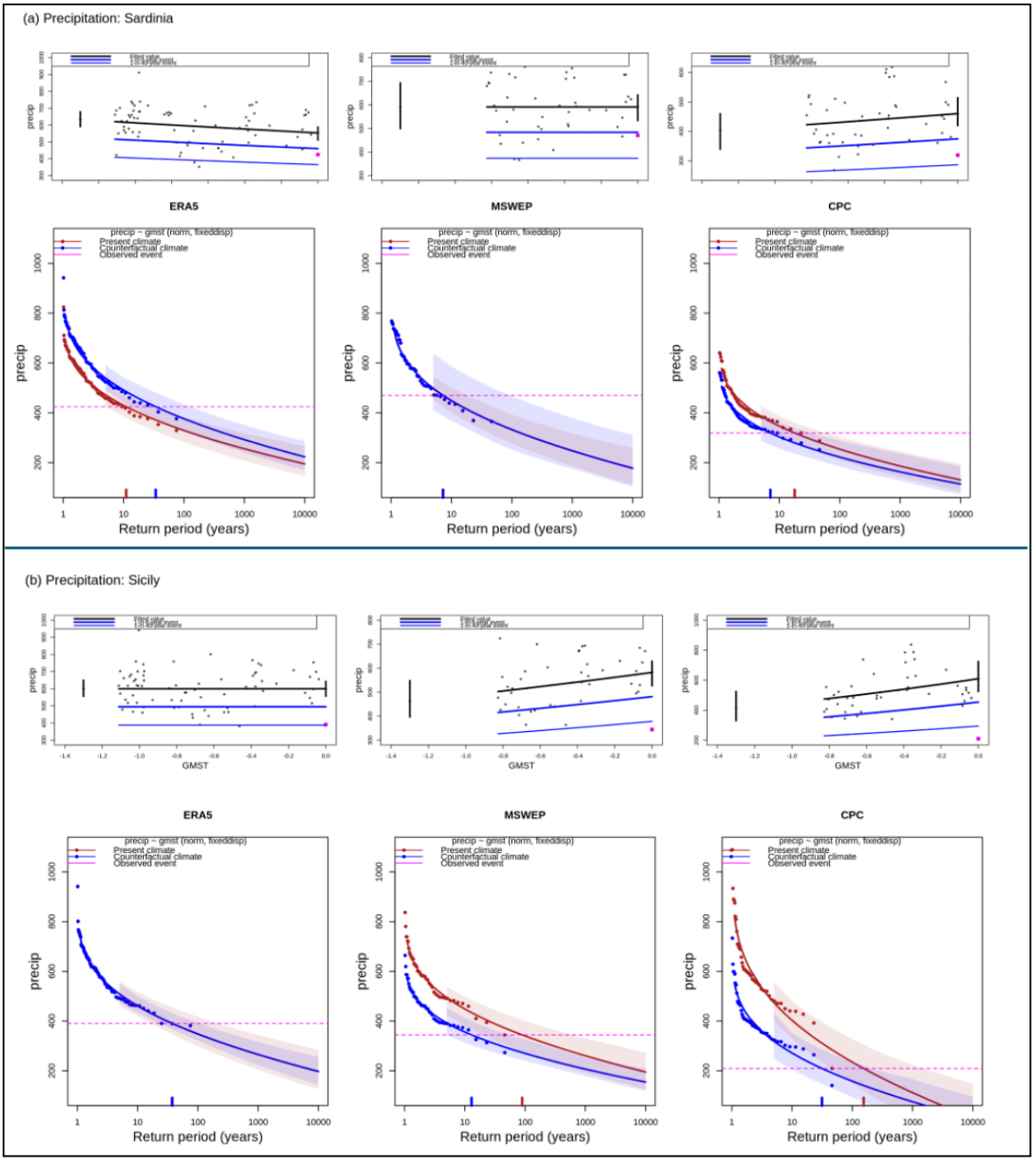

Figure 3.2. Same as Figure 3.1, for annual (Aug-July) precipitation over (a) Sardinia and , (b) Sicily.

3.1.3 Temperature

Unsurprisingly, both regions show an increase in annual temperature, in both the long and short datasets. The return period of the 2023/24 annual temperature is 130 years (32 -2000 years), 17 years (6.4 - 100) and 49 years (12 - 980) in the ERA5, MSWX and CPC datasets for Sardinia. Over Sicily, the return periods for the event are 270 years (64 - 8800), 73 years (14 - 1800) and 95 years (16 - 3100 years), in the respective datasets. In both regions, the return period is chosen as 100 years for defining the event for the attribution assessment. The probability ratios are very high with even the lowest bound>10000. Therefore reporting numbers is meaningless in this case, and we therefore simply state that, according to observations, temperatures such as this year would have been virtually impossible without climate change. The intensity changes due to global warming since pre-industrial times

estimated from ERA5, MSWX and CPC datasets are 2.1˚C (1.7 - 2.5˚C), 2.9 ˚C (2.2 - 3.5˚C) and 2/9˚C (2.2- 3.5˚C) in Sardinia and 1.7˚C (1.3 - 2.1˚C), 2.5˚C (1.9 - 3.2˚C) and 0.98˚C (0.19 - 1.7˚C) in Sicily.

We note that we also investigated the trends in PET in these datasets over the two regions- these are consistent and in line with temperature, which is the primary determinant of PET, and therefore not discussed again.

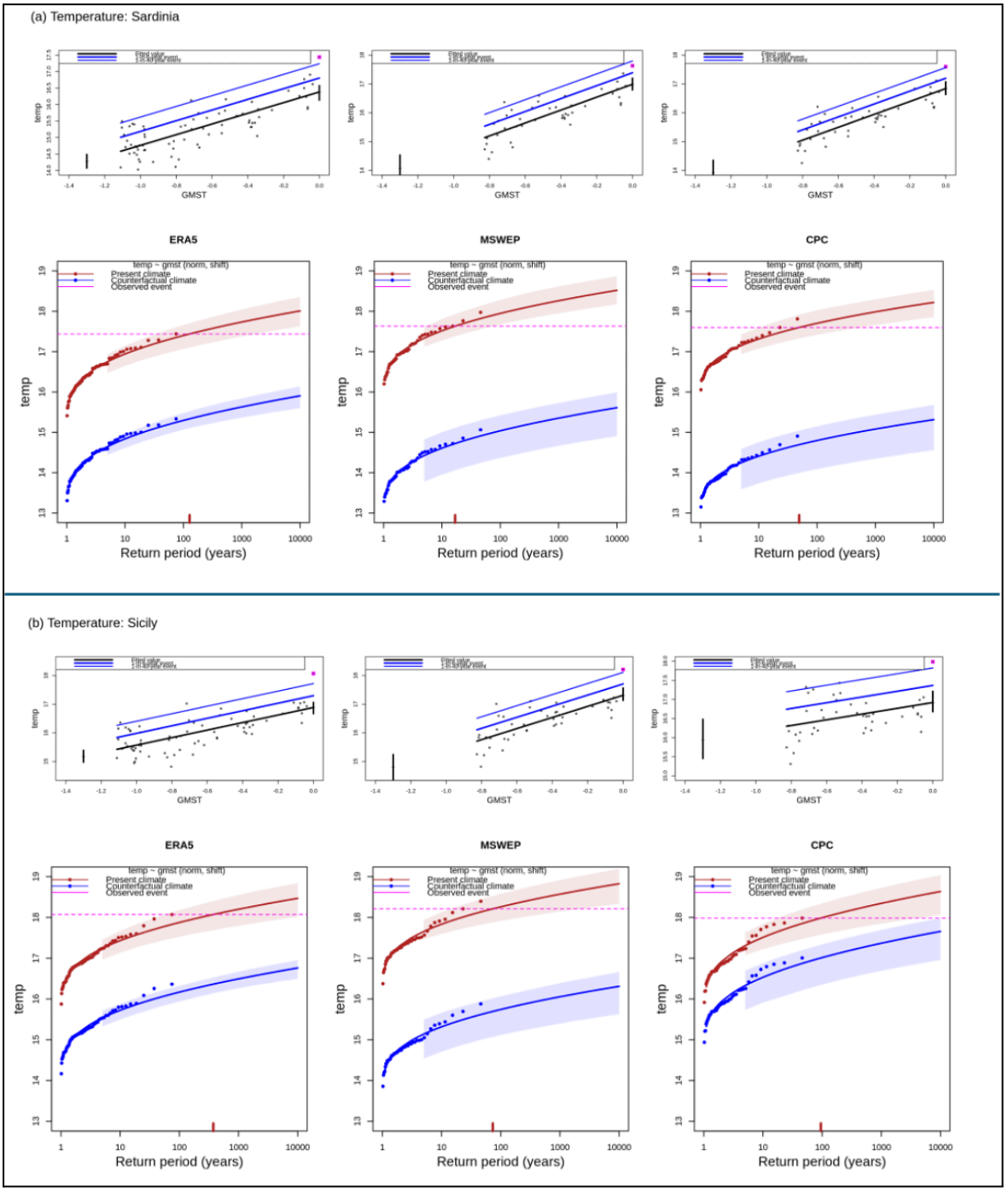

Figure 3.3. Same as Figure 3.1, for annual (Aug-July) temperature over (a) Sardinia and , (b) Sicily.

4 Model evaluation

In Tables 4.1 & 4.2 below, we show the results of the model evaluation for the Sardinia and Sicily regions, for August-July precipitation. The climate models are evaluated against the observations in their ability to capture the seasonal cycle and spatial pattern using CPC, ERA5, MSWEP and CHIRPS datasets as a reference. Models are also evaluated in terms of how well the statistical distribution of rainfall matches that of the observational datasets: if the best estimate of the scale parameter falls within the range of values estimated from the observations, the model is deemed 'good'; if the estimated confidence intervals overlap, the model is 'reasonable'; and if the confidence intervals do not overlap, the model is 'bad'. We rate the model as overall 'reasonable' or 'bad', if it is rated 'reasonable' or 'bad', respectively, for at least one criterion. If more than five models are rated 'good' for any framing, we use only the 'good' models in the attribution; otherwise we also include 'reasonable' models. We do not evaluate the models for the effective precipitation. We choose those models that pass the evaluation for precipitation for effective precipitation attribution analysis. Per framing or model setup we also use models that only just pass the evaluation tests if we only have five models or less for that framing that perform well.

Table 4.1. Evaluation results of the climate models considered for attribution analysis of August-July precipitation over the Sardinia region. For each model, the expected values of a 1-in-50 -year event is shown, along with the best estimate of the dispersion and the 95% confidence interval obtained via bootstrapping. Based on overall suitability, the models are classified as good, reasonable or bad, shown by green, yellow and red highlights, respectively.

Model / Observations	**Seasonal cycle**	**Spatial pattern**	**Dispersion**	**Event magnitude (mm)**
ERA5			0.18 (0.149 ... 0.206)	390.82
MSWEP			0.178 (0.135 ... 0.207)	344.447
CPC			0.264 (0.196 ... 0.323)	209.5101
				Magnitude of 100-year event (mm)
CORDEX				
CNRM-CM5_CCLM4-8-17	good	good	0.205 (0.157 ... 0.243)	410.090
CNRM-CM5_COSMO-crCLIM-v1-1	reasonable	good	0.221 (0.166 ... 0.261)	388.136
CNRM-CM5_REMO2015	bad	good	0.189 (0.122 ... 0.243)	442.855
CNRM-CM5_RegCM4-6	bad	reasonable	0.100 (0.0745 ... 0.122)	548.388
CNRM-CM5_KNMI-RACMO22E	reasonable	good	0.173 (0.134 ... 0.203)	576.894
EC-EARTH_COSMO-crCLIM-v1-1	reasonable	reasonable	0.225 (0.178 ... 0.260)	278.644
EC-EARTH_RACMO22E	good	reasonable	0.156 (0.110 ... 0.187)	467.902
HadGEM2-ES_CCLM4-8-17	reasonable	good	0.225 (0.166 ... 0.274)	309.907
HadGEM2-ES_COSMO-crCLIM-v1-1	good	good	0.267 (0.197 ... 0.321)	248.819
HadGEM2-ES_RegCM4-6	reasonable	good	0.159 (0.121 ... 0.186)	507.506
HadGEM2-ES_RACMO22E	good	good	0.202 (0.151 ... 0.236)	433.737
MPI-ESM-LR_CCLM4-8-17	reasonable	reasonable	0.181 (0.135 ... 0.207)	458.878
MPI-ESM-LR_COSMO-crCLIM-v1-1	good	reasonable	0.209 (0.155 ... 0.246)	385.700

MPI-ESM-LR_RegCM4-6	reasonable	reasonable	0.135 (0.0995 ... 0.161)	673.210
MPI-ESM-LR_RACMO22E	good	reasonable	0.159 (0.121 ... 0.187)	537.433
MPI-ESM-LR_REMO2009	reasonable	reasonable	0.172 (0.128 ... 0.202)	388.872
MPI-ESM-LR_WRF361H	reasonable	reasonable	0.177 (0.112 ... 0.216)	643.536
NorESM1-M_COSMO-crCLIM-v1-1	bad	reasonable	0.225 (0.161 ... 0.270)	250.237
NorESM1-M_-REMO2015	reasonable	reasonable	0.249 (0.173 ... 0.313)	206.464
NorESM1-M_RegCM4-6	good	reasonable	0.179 (0.136 ... 0.209)	550.909
NorESM1-M_RACMO22E	good	reasonable	0.192 (0.147 ... 0.222)	405.764

Table 4.2. Evaluation results of the climate models considered for attribution analysis of August-July precipitation over the Sicily region. For each model, the expected values of a 1-in-50 -year event is shown, along with the best estimate of the dispersion and the 95% confidence interval obtained via bootstrapping. Based on overall suitability, the models are classified as good, reasonable or bad, shown by green, yellow and red highlights, respectively.

Model / Observations	**Seasonal cycle**	**Spatial pattern**	**Dispersion**	**Event magnitude (mm)**
ERA5			0.18 (0.149 ... 0.206)	390.82
MSWEP			0.178 (0.135 ... 0.207)	344.447
CPC			0.264 (0.196 ... 0.323)	209.5101
				Magnitude of 100-year event (mm)
CORDEX				
CNRM-CM5_CCLM4-8-17	good	good	0.227 (0.135 ... 0.297)	189.130
CNRM-CM5_COSMO-crCLIM-v1-1	good	good	0.250 (0.187 ... 0.300)	213.996
CNRM-CM5_REMO2015	bad	good	0.246 (0.186 ... 0.286)	306.141
CNRM-CM5_RegCM4-6	bad	reasonable	0.153 (0.113 ... 0.178)	445.588
CNRM-CM5_KNMI-RACMO22E	reasonable	good	0.239 (0.192 ... 0.270)	358.864
EC-EARTH_COSMO-crCLIM-v1-1	reasonable	reasonable	0.343 (0.264 ... 0.390)	138.874
EC-EARTH_RACMO22E	reasonable	reasonable	0.238 (0.186 ... 0.279)	298.168
HadGEM2-ES_CCLM4-8-17	reasonable	good	0.274 (0.201 ... 0.317)	166.922
HadGEM2-ES_COSMO-crCLIM-v1-1	reasonable	good	0.308 (0.207 ... 0.364)	123.272
HadGEM2-ES_RegCM4-6	bad	good	0.183 (0.116 ... 0.225)	345.520
HadGEM2-ES_RACMO22E	good	good	0.224 (0.158 ... 0.277)	299.505
MPI-ESM-LR_CCLM4-8-17	good	reasonable	0.263 (0.194 ... 0.316)	265.972
MPI-ESM-LR_COSMO-crCLIM-v1-1	good	reasonable	0.291 (0.209 ... 0.350)	212.720
MPI-ESM-LR_RegCM4-6	reasonable	reasonable	0.163 (0.118 ... 0.198)	454.268
MPI-ESM-LR_RACMO22E	good	reasonable	0.256 (0.194 ... 0.294)	333.769
MPI-ESM-LR_REMO2009	reasonable	reasonable	0.312 (0.218 ... 0.383)	179.308
MPI-ESM-LR_WRF361H	reasonable	reasonable	0.246 (0.134 ... 0.307)	339.255
NorESM1-M_COSMO-crCLIM-v1-1	reasonable	reasonable	0.190 (0.145 ... 0.225)	126.196
NorESM1-M_-REMO2015	bad	reasonable	0.248 (0.181 ... 0.295)	149.506
NorESM1-M_RegCM4-6	reasonable	reasonable	0.175 (0.138 ... 0.203)	328.519

NorESM1-M_RACMO22E	reasonable	reasonable	0.184 (0.139 ... 0.216)	258.846

Multi-method multi-model attribution

This section shows Probability Ratios and change in intensity ΔI for models that passed the evaluation tests and also includes the values calculated from the fits with observations.

Table 5.1. Probability ratio and change in intensity of an event such as the recent 2023/24 August-July SPEI-12 due to changing GMST, for Sardinia: (a) from pre industrial climate to the present and (b) from the present to 2C above preindustrial.

	a. Past vs. present		**b. Present vs. future**	
Model / Observations	**Probability ratio PR [-]**	**Change in intensity ΔI [units]**	**Probability ratio PR [-]**	**Change in intensity ΔI [units]**
ERA5	50 (5.9 ... 1.1e+3)	-1.4 (-2.1 ... -0.68)		
ERA5-precal	1.6e+2 (16 ... 7.3e+3)	-1.6 (-2.4 ... -0.89)		
MSWEP	7.7 (0.39 ... 7.6e+2)	-0.84 (-2.0 ... 0.42)		
CNRM-CM5_CCLM4-8-17 ()	1.3 (0.33 ... 9.7)	-0.12 (-0.96 ... 0.70)	1.2 (0.80 ... 1.8)	-0.11 (-0.35 ... 0.11)
CNRM-CM5_COSMO-crCLIM-v1-1 ()	2.2 (0.46 ... 26)	-0.36 (-1.1 ... 0.43)	1.1 (0.73 ... 1.6)	-0.056 (-0.27 ... 0.16)
CNRM-CM5_KNMI-RACMO22E ()	0.70 (0.25 ... 4.6)	0.21 (-0.66 ... 1.0)	0.77 (0.45 ... 1.2)	0.15 (-0.12 ... 0.41)
EC-EARTH_COSMO-crCLIM-v1-1 ()	5.4 (1.2 ... 53)	-0.74 (-1.4 ... -0.10)	1.3 (0.95 ... 1.9)	-0.16 (-0.35 ... 0.030)
EC-EARTH_RACMO22E ()	1.6 (0.49 ... 8.0)	-0.25 (-0.90 ... 0.44)	1.0 (0.71 ... 1.5)	-0.021 (-0.22 ... 0.18)
HadGEM2-ES_CCLM4-8-17 ()	1.0 (0.40 ... 4.7)	-0.022 (-0.61 ... 0.51)	1.4 (1.1 ... 1.9)	-0.18 (-0.33 ... -0.038)
HadGEM2-ES_COSMO-crCLIM-v1-1 ()	1.3 (0.54 ... 4.8)	-0.13 (-0.59 ... 0.30)	1.2 (0.91 ... 1.6)	-0.087 (-0.22 ... 0.044)
HadGEM2-ES_RegCM4-6 ()	1.1 (0.34 ... 5.3)	-0.029 (-0.75 ... 0.67)	1.5 (1.1 ... 2.0)	-0.22 (-0.39 ... -0.035)
HadGEM2-ES_RACMO22E ()	0.79 (0.33 ... 2.7)	0.13 (-0.43 ... 0.69)	0.99 (0.72 ... 1.4)	0.0036 (-0.17 ... 0.17)
MPI-ESM-LR_CCLM4-8-17 ()	1.2 (0.36 ... 6.4)	-0.088 (-0.77 ... 0.65)	1.6 (1.2 ... 2.3)	-0.32 (-0.53 ... -0.095)
MPI-ESM-LR_COSMO-crCLIM-v1-1 ()	1.1 (0.37 ... 4.8)	-0.037 (-0.64 ... 0.54)	1.5 (1.1 ... 2.0)	-0.23 (-0.39 ... -0.057)
MPI-ESM-LR_RegCM4-6 ()	2.2 (0.47 ... 26)	-0.39 (-1.2 ... 0.42)	1.7 (1.1 ... 2.5)	-0.34 (-0.57 ... -0.075)
MPI-ESM-LR_RACMO22E ()	0.73 (0.28 ... 2.8)	0.17 (-0.43 ... 0.77)	1.3 (0.92 ... 1.8)	-0.14 (-0.32 ... 0.044)

MPI-ESM-LR_REMO2009 ()	1.8 (0.49 ... 10)	-0.32 (-1.0 ... 0.41)	1.6 (1.1 ... 2.3)	-0.30 (-0.54 ... -0.071)
MPI-ESM-LR_WRF361H ()	4.2e+4 (0.23 ... 5.0e+35)	-2.8 (-6.0 ... 0.97)	2.0 (0.79 ... 4.2)	-0.46 (-1.0 ... 0.13)
NorESM1-M_-REMO2015 ()	17 (2.4 ... 3.0e+2)	-1.0 (-1.7 ... -0.37)	1.8 (1.3 ... 2.5)	-0.33 (-0.52 ... -0.14)
NorESM1-M_RegCM4-6 ()	0.71 (0.20 ... 7.9)	0.18 (-0.81 ... 1.2)	1.1 (0.73 ... 1.8)	-0.071 (-0.31 ... 0.16)

Table 5.2. Probability ratio and change in intensity of an event such as the recent 2023/24 August-July SPEI-12 due to changing GMST, for Sicily: (a) from pre industrial climate to the present and (b) from the present to 2C above preindustrial.

	a. Past vs. present		**b. Present vs. future**	
Model / Observations	**Probability ratio PR [-]**	**Change in intensity ΔI [units]**	**Probability ratio PR [-]**	**Change in intensity ΔI [units]**
ERA5	3.7 (0.31 ... 49)	-0.40 (-1.1 ... 0.32)		
ERA5-precal	13 (1.2 ... 2.4e+2)	-0.78 (-1.5 ... -0.053)		
MSWEP	0.062 (0.000066 ... 5.3)	0.86 (-0.53 ... 2.1)		
CNRM-CM5_CCLM4-8-17 ()	1.7 (0.24 ... 24)	-0.17 (-0.88 ... 0.57)	1.7 (0.88 ... 3.1)	-0.22 (-0.46 ... 0.050)
CNRM-CM5_ETH-COSMO-crCLIM-v1-1 ()	1.8 (0.24 ... 20)	-0.20 (-0.89 ... 0.51)	1.5 (0.80 ... 2.9)	-0.16 (-0.40 ... 0.083)
CNRM-CERFACS-CNRM-CM5_KNMI-RACMO22E ()	0.67 (0.098 ... 10)	0.14 (-0.69 ... 0.95)	0.94 (0.45 ... 1.7)	0.022 (-0.21 ... 0.27)
EC-EARTH_CLMcom-ETH-COSMO-crCLIM-v1-1 ()	4.8 (0.72 ... 90)	-0.48 (-1.1 ... 0.11)	1.4 (0.89 ... 2.3)	-0.11 (-0.28 ... 0.039)
EC-EARTH_RACMO22E ()	1.8 (0.32 ... 20)	-0.18 (-0.82 ... 0.39)	0.87 (0.50 ... 1.5)	0.045 (-0.13 ... 0.21)
HadGEM2-ES_CCLM4-8-17 ()	2.2 (0.44 ... 23)	-0.25 (-0.82 ... 0.30)	1.0 (0.64 ... 1.6)	0.00082 (-0.16 ... 0.15)
HadGEM2-ES_COSMO-crCLIM-v1-1 ()	6.9 (1.0 ... 80)	-0.53 (-1.0 ... -0.015)	0.93 (0.60 ... 1.5)	0.022 (-0.12 ... 0.16)
HadGEM2-ES_RACMO22E ()	1.1 (0.24 ... 8.2)	-0.044 (-0.68 ... 0.57)	1.0 (0.64 ... 1.6)	-0.0025 (-0.18 ... 0.16)
MPI-ESM-LR_CCLM4-8-17 ()	1.1 (0.21 ... 8.2)	-0.034 (-0.55 ... 0.54)	1.7 (1.0 ... 2.7)	-0.18 (-0.35 ... -0.0013)
MPI-ESM-LR_COSMO-crCLIM-v1-1 ()	1.2 (0.27 ... 8.0)	-0.047 (-0.52 ... 0.44)	1.9 (1.2 ... 3.3)	-0.23 (-0.40 ... -0.051)
MPI-ESM-LR_RegCM4-6 ()	0.65 (0.095 ... 7.1)	0.15 (-0.58 ... 0.93)	2.1 (1.1 ... 3.9)	-0.28 (-0.52 ... -0.044)
MPI-ESM-LR_RACMO22E ()	0.51 (0.14 ... 2.4)	0.23 (-0.27 ... 0.79)	1.5 (0.93 ... 2.4)	-0.15 (-0.30 ... 0.026)

MPI-M-MPI-ESM-LR_MPI-CSC-REMO2009 ()	1.9 (0.36 ... 13)	-0.20 (-0.66 ... 0.33)	2.2 (1.4 ... 3.6)	-0.28 (-0.44 ... -0.12)
MPI-M-MPI-ESM-LR_UHOH-WRF361H ()	7.0e+6 (5.1 ... 1.6e+26)	-2.7 (-6.1 ... -0.40)	3.8 (1.1 ... 12)	-0.52 (-1.0 ... -0.023)
NorESM1-M_COSMO-crCLIM-v1-1 ()	16 (1.4 ... 4.6e+2)	-0.85 (-1.6 ... -0.11)	2.2 (1.2 ... 3.9)	-0.28 (-0.49 ... -0.067)
NorESM1-M_RegCM4-6 ()	5.5 (0.33 ... 2.7e+2)	-0.51 (-1.4 ... 0.38)	1.1 (0.52 ... 2.2)	-0.026 (-0.27 ... 0.21)

Appendix tables Table A.1-A.4 shows the PRs and intensity changes in annual (Aug-July) precipitation and temperature area-averaged over the study regions.

6 Hazard synthesis

We evaluate the influence of anthropogenic climate change on drought as defined by SPEI12 in Sardinia and Sicily by calculating the probability ratio as well as the change in intensity using observations and climate models. We also do the same for precipitation and temperature over the same timeframe and both islands to understand the meteorological drivers of the observed changes in drought intensity and likelihood. We only include models that pass the evaluation described above in the analysis. The aim is to synthesise results from models that pass the evaluation along with the observations-based products, to give an overarching attribution statement. Figs. 6.1-6.4 show the changes in probability and intensity for the observations (blue) and models (red). Before combining them into a synthesised assessment, first, a representation error is added (in quadrature) to the observations, to account for the difference between observations-based datasets that cannot be explained by natural variability. This is shown in these figures as white boxes around the light blue bars. The dark blue bar shows the average over the observation-based products. Next, a term to account for intermodel spread is added (in quadrature) to the natural variability of the models. This is shown in the figures as white boxes around the light red bars. The dark red bar shows the model average, consisting of a weighted mean using the (uncorrelated) uncertainties due to natural variability plus the term representing intermodel spread (i.e., the inverse square of the white bars). Observation-based products and models are combined into a single result in two ways. Firstly, we neglect common model uncertainties beyond the intermodel spread that is depicted by the model average, and compute the weighted average of models (dark red bar) and observations (dark blue bar): this is indicated by the magenta bar. As, due to common model uncertainties, model uncertainty can be larger than the intermodel spread, secondly, we also show the more conservative estimate of an unweighted, direct average of observations (dark red bar) and models (dark blue bar) contributing 50% each, indicated by the white box around the magenta bar in the synthesis figures.

For Sardinia, the observations show a much stronger increase in intensity and likelihood of droughts than the models, so the weighted synthesis, with an increase in likelihood of a factor of 1.40 (0.802 - 2.63) and the intensity change of -0.224 (-0.461 - 0.0122), which means the synthesised results for the region which suggests that the 1-in-10 year ‘extreme’ drought (D3) would be a milder moderate drought (D1) without climate change, is a conservative estimate. The unweighted mean indicates a much higher upper bound. That this is indeed a conservative estimate is further corroborated by analysing precipitation and temperature, the main driver of PET separately. Here we see (Figures A1-A4) no change in likelihood and intensity for rainfall in the observations as well as the models in precipitation. The overall synthesised results for precipitation over Sardinia gives a PR= 1.2 (0.8 - 1.9) and intensity change of 2.5% decrease (9.5% decrease - 4.8% increase). A much stronger increase in temperature is seen in the observations as compared to models, with best estimated

intensity changes of 2.64C in the observations and 1.4C in the models. This problem of trends in temperatures being underestimated by climate models is a well known problem (van Oldenborgh et al., 2022) and suggests the SPEI12 results from the models are indeed too conservative.

For Sicily the picture would look similar if it wasn't for the observations based product CPC, that shows an opposing signal compared to all other products, what we find for Sardinia and what we would expect in a warming climate. While this means that overall the synthesised changes are smaller for Sicily, with respect to the intensity change of -0.191 (-0.456 - 0.0757), the 100-year drought in today's climate that is an 'extreme' drought in the observations (D3) would be milder without climate change and classified as a 'severe' drought (D2). The likelihood change is with a factor of 1.88 (0.755 - 4.95) slightly higher than for Sardinia but with a larger uncertainty. Due to the strange behaviour of CPC we don't see the discrepancy between observations and models that is visible for Sardinia. This picture is the same when looking at changes in temperature, where CPC also shows a much lower trend compared to the other observational data sets, more comparable with model trends. Given that there is no explanation for the differences, and from a physical point of view we do expect higher temperature to result in higher PET and thus lower SPEI12 values with no change in rainfall due to climate change, we do not trust the numerical values from the synthesis in the case of Sicily and report that the changes in likelihood are comparable to those in Sardinia giving an increase of about 50%.

This assessment is supported by the analysis of future changes in SPEI12 which show an increase in likelihood and intensity in both regions under a further 0.7C warming, compared to today's climate.

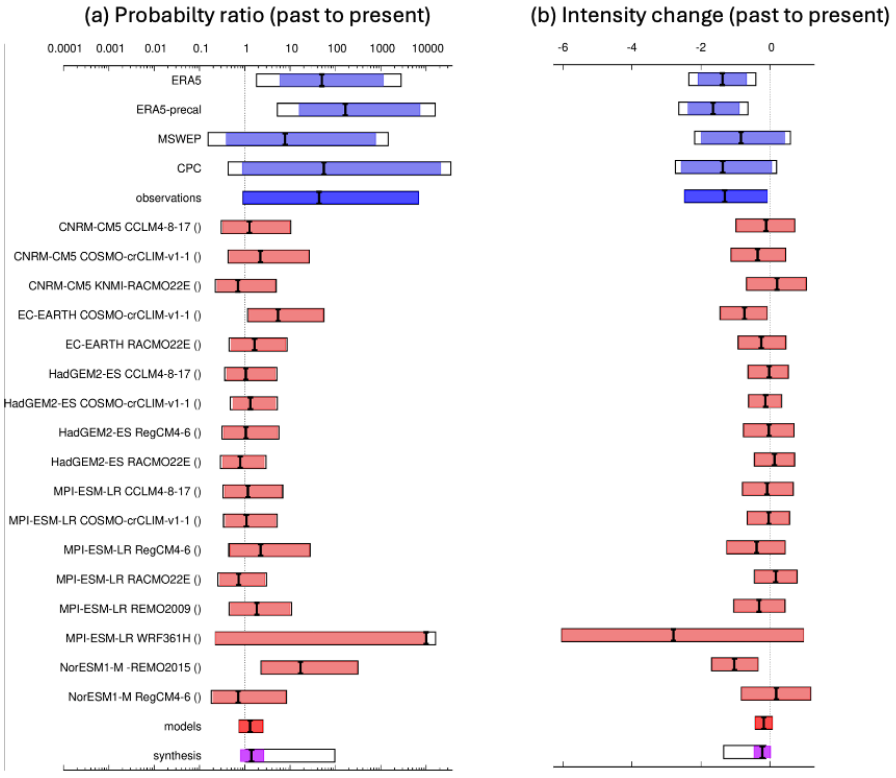

Figure 6.1. (left) Synthesis of probability ratios and (right) intensity changes in SPEI units, when comparing the return period and magnitudes of the SPEI-12 in July over Sardinia in the current climate and a 1.3°C cooler climate.

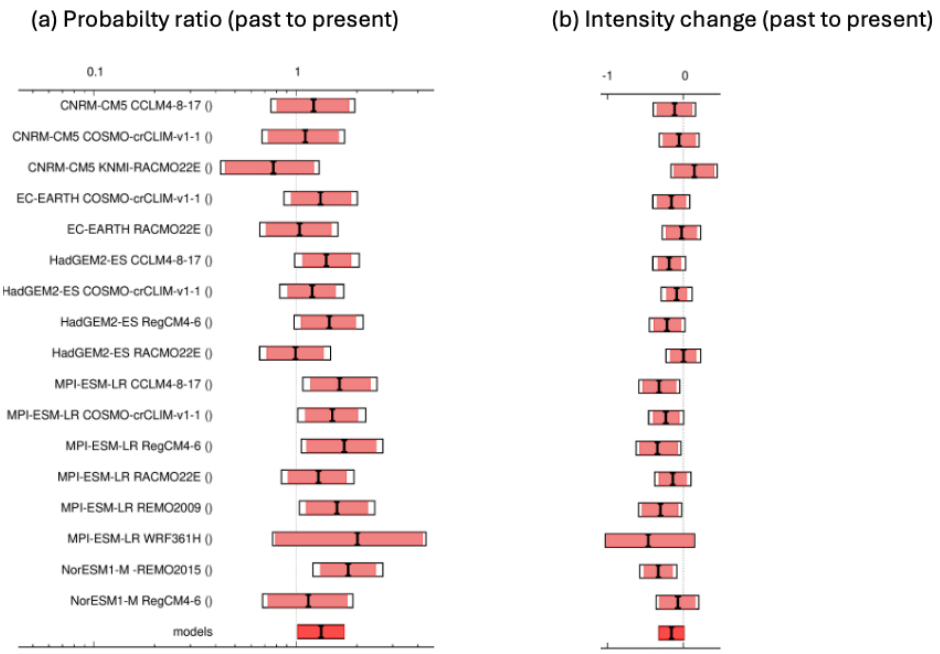

Figure 6.2. (left) Synthesis of probability ratios and (right) intensity changes in SPEI units, when comparing the return period and magnitudes of the SPEI-12 in July over Sardinia in the current climate and in a further 0.7°C warmer climate.

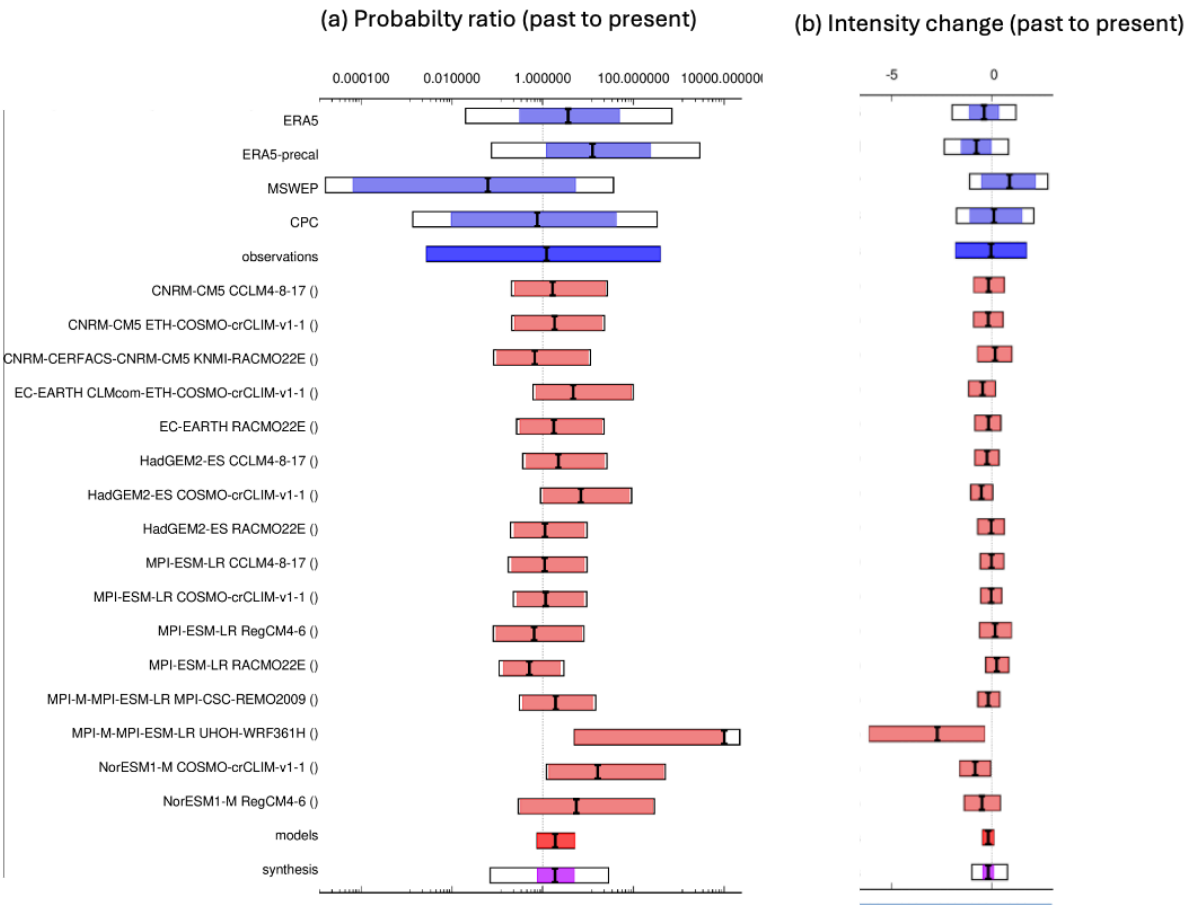

Figure 6.3. Same as Fig. 6.1, for Sicily

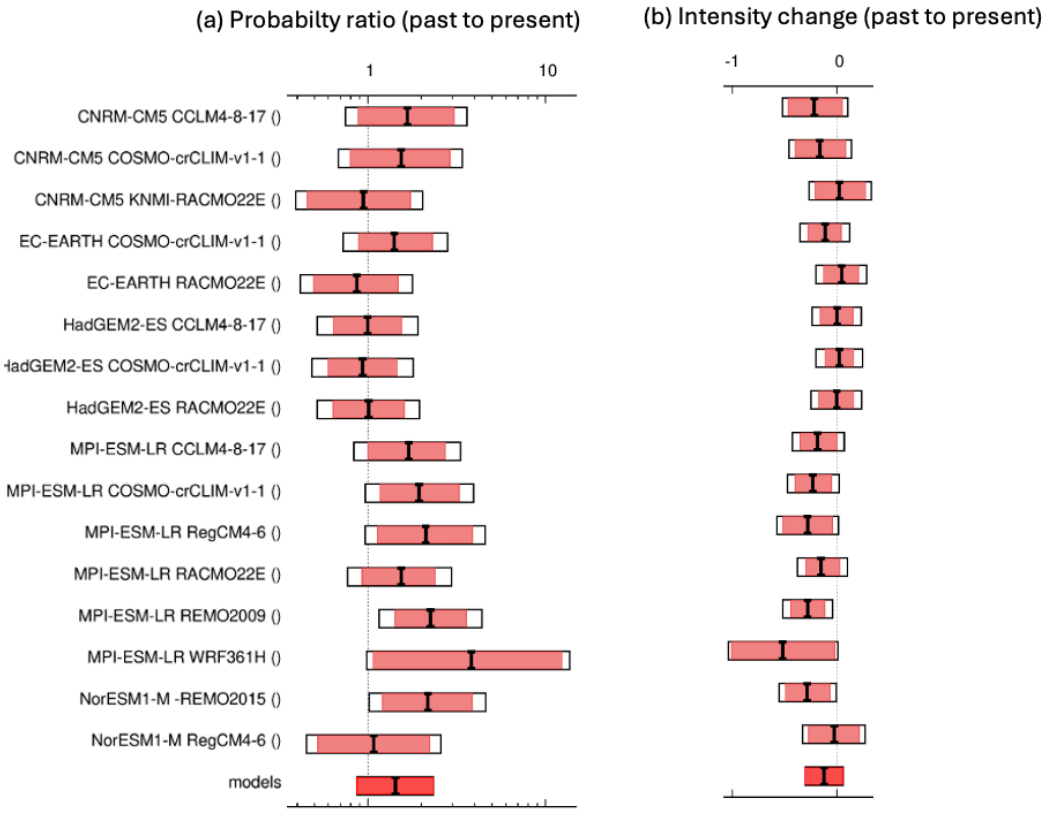

Figure 6.4. Same as Fig. 6.2, for Sicily

7 Vulnerability and exposure

Affected by prolonged meteorological drought, Sicily and Sardinia both experience cascading impacts on human health, water resources, agriculture, and tourism. While water scarcity has long been a significant challenge (Cangemi et al., 2019; Sirigu & Montaldo, 2022), the coupling of heat and wildfires with drought conditions has escalated water demand across all sectors, further straining the limited resources (Leon et al., 2022).

Agriculture and tourism play a dual role in the drought and water crisis in Sicily and Sardinia. On one hand, they significantly drive water consumption, exacerbating water scarcity, while on the other hand, they are highly vulnerable to the impacts of water shortages (Mereu et al., 2013). The islands rely heavily on winter precipitation stored in reservoirs to meet their water demands for agriculture and tourism, however, with reservoirs running dry (Copernicus, 2024), the islands are experiencing considerable stress on their water supply systems, leading to widespread water rationing (Duello, 2024; Dongo, 2024). In Sicily, the drought has inflicted an estimated 2.7 billion euros in damages, highlighting the severe economic impacts (RTL Today, 2024). On 6 May and 30 July, respectively, Sicily and Sardinia declared states of emergency, due to emergencies in relation to the water deficits (Euro News, 2024; Duello, 2024).

7.1 Water systems

Sicily's water system, serving approximately 5 million residents, relies on surface water from reservoirs and artificial basins, as well as groundwater from aquifers. The infrastructure includes dams, reservoirs, and a distribution network of pipes, with some underground aqueducts dating back to ancient times. This historically developed system faces significant challenges, including aging infrastructure, high water losses, and inefficient distribution. According to the Italian National Institute of Statistics (ISTAT), in 2022, Sicily experienced a 51.6% water loss during the introduction of water into the network, amounting to 339.7 million cubic meters of wasted water (ISTAT, 2024). Recent updates have been limited, leaving the system strained by ongoing droughts. The current state of Sicilian reservoirs is concerning, as their capacity is severely hindered by sediment accumulation (Musumeci, 2023). This degradation hampers their ability to effectively manage flood control and to act as reliable water reserves for the region.

In Sardinia, the water system supports about 1.6 million residents, and the island's water supply system is a blend of sources. Approximately 57% of the water supply is derived from surface water, primarily from the island's three main rivers (the Tirso, Flumendosa, and Coghinas), which is stored and regulated by an extensive network of reservoirs (ISRI, 2008). Notably, the Tirso River was dammed in 1923 to create Lake Omodeo, which, at 22 km², is the largest artificial lake in Italy (ISRI, 2008). The remaining 43% comes from underground water sources, tapping into the various aquifers located beneath the surface (ISRI, 2008).

Sardinia stands out as the Italian region where extraordinary engineering efforts for watercourse regulation have been realized, primarily through the construction of dams and artificial basins. These monumental structures are integral to managing water resources on the island. Beyond dams, the water system infrastructure comprises pumping stations, hydroelectric power stations, and a water distribution network monitored by a satellite communication system since 2005. The system has seen updates, including the implementation of smart water meters in 2022, aimed at reducing non-revenue water. Despite these efforts, challenges persist, particularly regarding high water losses and aging infrastructure. In 2022, ISTAT identified a 52.8% water loss through the water distribution system on the island (ISTAT, 2024). Additionally, while surface water sources fulfill about three-fifths of the total regional water demand, they often struggle with quality issues. This is largely attributed to pollution stemming from substandard sewage systems, insufficient treatment facilities, and the overapplication of nutrients within agricultural practices. Conversely, underground water sources, although limited in quantity, are crucial for meeting local needs. Their reliability is challenged by a concerning trend of aquifer salinization that has developed in recent years, further complicating water resource management on the island.

The disappearance of Lake Pergusa and the alarming conditions of other reservoirs across Sicily (such as the Fanaco, Ogliastro, Pozzillo, and Disueri lakes) highlight the dire state of the island's water resources (Duello, 2024). As of early 2024, severe water shortages have necessitated rationing across over 50 municipalities in Sicily. In Sardinia, the situation is similarly bleak, with water reserves such as Lake Alto del Flumendosa reduced to less than 50% of their capacity, necessitating strict water usage restrictions (see figure 7.1) (Copernicus, 2024; Yahoo, 2024). A striking example of the severity of this situation is found in the Posada district, where irrigation has been prohibited to prioritize the availability of potable water. The combination of ineffective water systems and increasing drought

conditions underscores the urgent need for integrated management and infrastructural renewal to mitigate water scarcity in these regions.

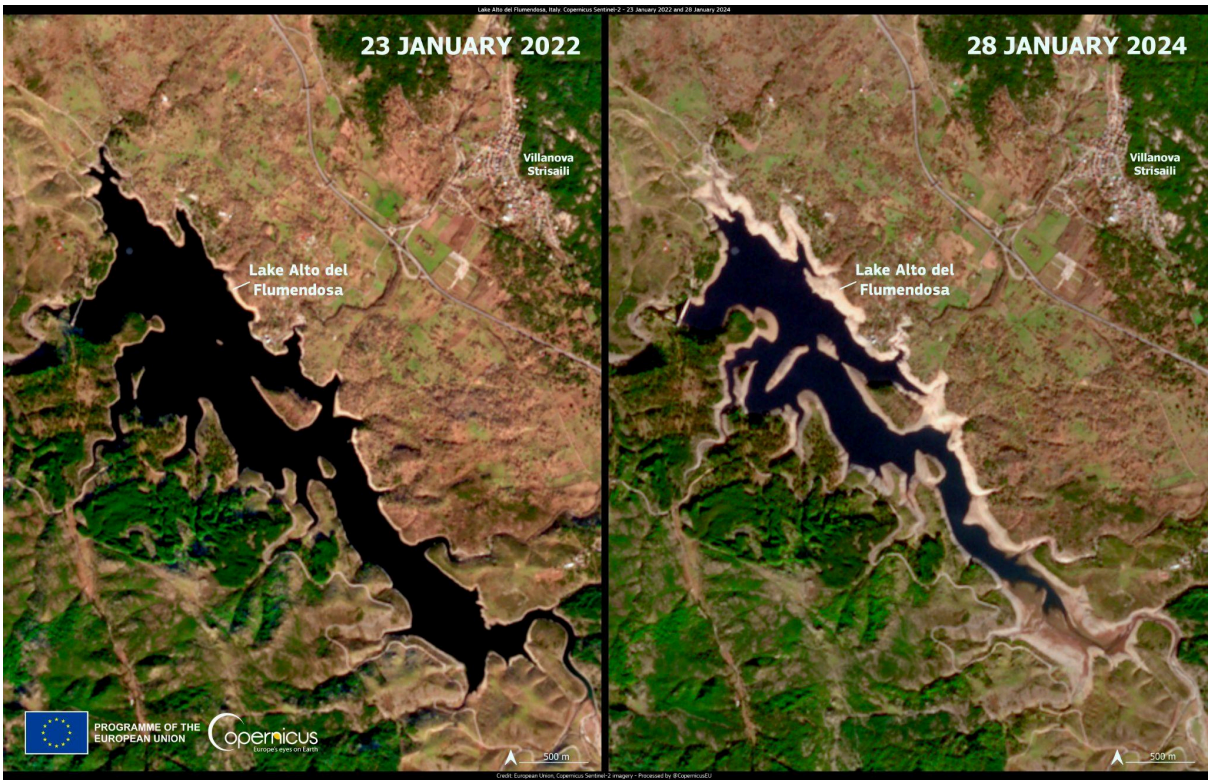

Figure 7.1. *Satellite images of Lake Alto del Flumendosa, demonstrating a considerable decrease in water level between 23 Junaury, 2022, and 28 january, 2024. Source: European Union, Copernicus Sentinel-2 Imagery (2024).*

7.2 Agriculture

Agriculture occupies approximately 44 and 68.5% of Sardinia and Sicily's land, respectively, and it includes livestock farming, crop cultivation (e.g. grains, vegetables, and fruits), and specialized agriculture (notably cork) (European Commission, 2023; European Commission, 2024). In Sicily, agricultural land has expanded by 50 hectares per year since 1990, resulting in a 62% decrease in both natural and semi-natural ecosystems (Ferrarini et al., 2021). On both islands, recent developments have focused on organic conversion and maintenance, prioritizing the promotion of quality products. Despite simultaneous modernization, water demand is increasing. At the same time, the agricultural sectors' economic contributions remain relatively low (Mereu et al., 2013; European Commission, 2023; European Commission, 2024), and constrained by factors including poor soil quality and small farm sizes. However, it is important to note that it supports people's livelihoods.

The ongoing drought exacerbates the vulnerability of agricultural systems, especially for small-scale farmers and pastoralists, who face severe crop and livestock losses (Duello, 2024; Santalucia, 2024; Ruffino, 2024). In Sicily, farmers have been forced to uproot citrus groves, slaughter animals, and rely on costly private water tankers to sustain livestock (Symons, 2024; Duello, 2024; Ruffino, 2024), while olives are falling prematurely in some regions months ahead of harvest (DeAndreis, 2024). In

the hardest-hit areas, grain and forage harvests have dwindled to nearly zero, creating a domino effect of economic losses that threaten the closure of agricultural enterprises (Duello, 2024).

Interventions are crucial, but they face significant challenges. While plans to increase irrigation have been proposed to boost agricultural viability, they risk further straining already scarce water resources. The projected increase in irrigation demand, compounded by rising temperatures and extreme climate events, threatens to outpace the capacity of existing water systems, highlighting the need for alternative water sources and more efficient water management (Mereu et al., 2013).

Social capital and local knowledge play important roles in mitigating drought impacts. For instance, agroecological practices, which emphasize resilience through farmers' knowledge and community participation, offer promising solutions. However, these approaches struggle due to unfavorable socio-political conditions and the dominance of industrialized agribusiness systems, which rely on seasonal migrant workers and perpetuate social inequities (Conte et al., 2024).

7.3 Tourism

Being a key sector on both islands, tourism substantially contributes to the regional economy (Köberi et al., 2015). However, its seasonal nature, concentrated during the dry summer months, intensifies water demand precisely when water availability is at its lowest. Tourists tend to use more water during their stays compared to local residents, driven by the need for amenities such as swimming pools, landscaped gardens, and other water-intensive services provided by hotels and resorts (Köberi et al., 2015). The increased water consumption during peak tourist seasons puts severe pressure on the already limited water resources, competing with the needs of local residents, and agriculture (Mereu et al., 2013).

The strain on water resources due to tourism has had tangible consequences. In some instances, Sicilian cities have been forced to turn away tourists due to the inability to guarantee basic water-dependent amenities, such as showers and flushing toilets (Prakash, 2024; Nadeau, 2024). This situation is particularly critical in areas like Agrigento, where hoteliers report a wave of cancellations due to water shortages (Duello, 2024).

Moreover, the tourism industry’s reliance on consistent water availability makes it vulnerable to climate-induced changes. The sector’s growth under scenarios of increased drought frequency could lead to a doubling of water demands (Mereu et al., 2013), necessitating significant investments in water infrastructure and potentially heightening tension with other water users. Thus, while tourism drives water scarcity, it is also at considerable risk from the very crisis it helps to exacerbate.

7.4 Drought risk management and policies

Italy has had multiple severe droughts over the past century. As a response to these, various drought risk management and policies have been put into place, which Rossi (2020) comprehensively summarizes. For example, several drought monitoring systems which produce bulletins have been set up, including Sicily (Rossi & Cancelliere, 2002) and other Italian regions. However, for many years,

the government has mostly had a reactive response to drought (Rossi, 2020). This response focussed mostly on 1) emergency actions, and 2) subsidies to farmers for covering agricultural damages (ibid.).

The Drought Early Warning Systems in Sardinia and Sicily, managed by the Civil Protection Service, operate through a multi-tiered structure. This includes data collection and analysis via the Copernicus Drought Observatory and the respective Regional Agencies for Environmental Protection. These agencies are responsible for monitoring drought conditions and issuing impact-based forecast bulletins.

To understand the functioning of the Civil Protection Service in this context, one can examine two key elements: the Drought Report of the Sicilian Region (such as the one available at Regione Siciliana Drought Report) and the Sardinian region's bulletins. By cross-referencing these documents with the subsequent response actions, is it possible to gain insights into the regional approaches to drought management. For example, in Sardinia, the Civil Protection Ordinance No. 1, issued on 5 August 2024 and titled "Initial urgent measures and delineation of the territory affected by the current water deficit in the Sardinia Region," specifies the response actions within a multi-hazard context. Municipalities are responsible for identifying farms experiencing water shortages and for coordinating the delivery of water via tankers, pending the full implementation of services outlined in Article 2 of the Ordinance. These requests are then relayed to the Regional Integrated Operations Centre (SORI), which deploys resources from the Forestas Agency and civil protection volunteer organisations, following the established protocol for "Activation of the regional civil protection system for water supply with tankers. This strategy is tailored to address the region's multi-hazard challenges, with a specific emphasis on wildfire risks. The ordinance clearly states that water supply operations will be suspended on days when the "Fire Danger Forecast Bulletin" signals an extreme hazard level (Code Red) for the relevant municipality, or when a pre-alert status is declared. Moreover, the Forestry Corps and Environmental Vigilance (CFVA) are authorised to prioritise the allocation of tankers for firefighting efforts through the Operational Centres (COP) if the situation demands it.

As a result of a Guidance Document on drought preparedness and mitigation prepared by the EU Water Scarcity and Drought Expert Network (European Commission, 2007), a shift took place in Italy to go from emergency management to more preventative policies. In more recent years, drought management has been covered in national legislation. Decree Law No. 39 of April 14, 2023, which was converted into Law No. 68/2023 (Official Journal No. 136 on June 13, 2023), includes measures to address water scarcity and strengthen water infrastructure. Efforts have also been made to improve data collection on water supplies and agricultural damages (Baldwin & Casalini, 2021). Since 2016, Observatories on water resources have been established, aimed at drought and water scarcity monitoring and the regulation of water resources management during drought events (ISPRA, 2018; Rossi, 2020). Italy's National Adaptation Plan, approved in December 2023, includes a database of adaptation actions and a list of relevant national/regional/local norms and policies (ClimateADAPT, n.d.).

During this drought event, already in February, heavy water rationing was put in place across over 90 communities in Sicily. In some of the most affected areas, it was reported that water was only running every 15 days, which led to multiple protests (Pereira, 2024). Although people were warned about water cuts, some cases were reported of individuals who did not receive warnings ahead of time

(ibid.). Furthermore, some local populations mentioned they already saw the drought coming during the autumn last year, due to almost zero rainfall and high temperatures (Duello, 2024).

On May 6, the national government declared a state of emergency in Sicily, partly to manage resources until autumn. The government allocated €20 million for the purpose of buying water tankers, digging new wells, and fixing aqueducts (Santalucia, 2024a). The regional government allocated subsidies for farmers forced to buy hay from third parties. The Sicilian region also allocated €90 million to reactivate three desalination plants that were previously abandoned for many years (Toreti et al., 2024). In late July, an Italian navy tanker ship arrived in Licata to supply 1,2 million liters of water to the most affected areas and residents (Santalucia, 2024b). The supply of water via the tanker was costly, at €43 per cubic metre. Pending a cost verification and alternative solutions, the service is temporarily suspended while other supply sources are being explored (Proteziona Civile Regione Siciliana, 2024).

Within this operational framework, the Italian Red Cross serves as an Operational Structure of the National Civil Protection Service, engaging in various roles. For instance, in Sicily, the Red Cross has been involved in the Local Coordination, such as in Messina, or distributed water to the population, as seen, for example, in Caltanissetta.

7.5 V&E conclusions

Drought impacts in Sardinia and Sicily are compounded by simultaneous wildfires and extreme heat. The current drought has an impact on, and is mediated by water demands in many sectors, including agriculture and tourism, in addition to the daily need of the population. The existing water management systems are severely impacted by the drought, and are not resilient to changes in rainfall driven by climate change that Sardinia and Sicily are already experiencing. Effective drought risk management in regions such as Sardinia and Sicily requires a sustained focus on long-term preparedness and adaptation. Investing in resilient infrastructure, water conservation strategies, and sustainable resource management is crucial to mitigating the impacts of drought.

Data availability

Almost all data is available via the Climate Explorer. For more information, contact wwamedia@imperial.ac.uk

Appendix

Table A.1. Probability ratio and change in intensity of an event such as the recent 2023/24 August-July low precipitation due to changing GMST, for Sardinia: (a) from pre industrial climate to the present and (b) from the present to 2C above preindustrial.

	a. Past vs. present		**b. Present vs. future**	
Model / Observations	**Probability ratio PR [-]**	**Change in intensity ΔI [units]**	**Probability ratio PR [-]**	**Change in intensity ΔI [units]**

ERA5	3.1 (1.1 ... 12)	-13 (-24 ... -1.0)		
ERA5-precal	1.0 (0.22 ... 8.0)	-0.0097 (-22 ... 26)		
MSWEP	0.39 (0.054 ... 1.9)	14 (-7.9 ... 51)		
CNRM-CM5_CCLM4-8-17 ()	1.0 (0.34 ... 3.6)	0.043 (-16 ... 18)	1.1 (0.84 ... 1.5)	-1.6 (-6.7 ... 2.6)
CNRM-CM5_COSMO-crCLIM-v1-1 ()	1.1 (0.36 ... 6.1)	-0.95 (-18 ... 17)	0.95 (0.69 ... 1.3)	0.85 (-3.5 ... 5.5)
CNRM-CM5_KNMI-RACMO22E ()	0.73 (0.25 ... 3.2)	3.8 (-12 ... 20)	0.74 (0.50 ... 1.0)	3.5 (-0.30 ... 7.3)
EC-EARTH_COSMO-crCLIM-v1-1 ()	2.5 (1.1 ... 7.5)	-14 (-27 ... -1.6)	1.2 (0.93 ... 1.6)	-3.1 (-8.0 ... 1.2)
EC-EARTH_RACMO22E ()	1.6 (0.69 ... 4.5)	-5.3 (-14 ... 4.7)	1.0 (0.81 ... 1.4)	-0.55 (-4.0 ... 2.5)
HadGEM2-ES_CCLM4-8-17 ()	1.0 (0.43 ... 2.6)	0.080 (-15 ... 15)	1.2 (1.0 ... 1.5)	-4.1 (-8.6 ... -0.26)
HadGEM2-ES_COSMO-crCLIM-v1-1 ()	1.3 (0.68 ... 2.6)	-6.4 (-19 ... 9.0)	1.2 (1.0 ... 1.4)	-4.0 (-8.9 ... 0.055)
HadGEM2-ES_RegCM4-6 ()	1.1 (0.39 ... 3.7)	-0.59 (-13 ... 12)	1.4 (1.1 ... 1.8)	-4.0 (-7.3 ... -0.65)
HadGEM2-ES_RACMO22E ()	0.80 (0.36 ... 1.9)	3.8 (-9.4 ... 18)	0.95 (0.76 ... 1.2)	0.85 (-3.3 ... 4.3)
MPI-ESM-LR_CCLM4-8-17 ()	0.94 (0.37 ... 3.2)	0.86 (-12 ... 15)	1.3 (1.0 ... 1.8)	-4.6 (-9.0 ... -0.32)
MPI-ESM-LR_COSMO-crCLIM-v1-1 ()	0.94 (0.43 ... 2.3)	0.95 (-11 ... 13)	1.3 (0.98 ... 1.7)	-4.3 (-9.0 ... 0.39)
MPI-ESM-LR_RegCM4-6 ()	1.7 (0.58 ... 8.4)	-4.6 (-15 ... 4.9)	1.5 (1.0 ... 2.1)	-4.3 (-8.2 ... -0.32)
MPI-ESM-LR_RACMO22E ()	0.70 (0.30 ... 1.9)	4.0 (-5.9 ... 14)	1.2 (0.92 ... 1.5)	-1.9 (-5.2 ... 1.0)
MPI-ESM-LR_REMO2009 ()	1.7 (0.62 ... 5.1)	-7.3 (-20 ... 5.9)	1.3 (1.0 ... 1.9)	-5.2 (-11 ... 0.023)
MPI-ESM-LR_WRF361H ()	13 (0.75 ... 2.3e+6)	-26 (-63 ... 3.8)	1.5 (0.72 ... 3.3)	-7.5 (-20 ... 4.8)
NorESM1-M_-REMO2015 ()	4.1 (1.4 ... 15)	-25 (-38 ... -6.2)	1.5 (1.3 ... 1.9)	-10 (-15 ... -4.7)
NorESM1-M_RegCM4-6 ()	0.67 (0.20 ... 4.4)	5.4 (-14 ... 28)	1.1 (0.80 ... 1.6)	-1.4 (-6.1 ... 2.6)
NorESM1-M_RACMO22E ()	1.6 (0.54 ... 7.1)	-5.9 (-19 ... 9.1)	1.2 (0.93 ... 1.6)	-2.7 (-6.1 ... 0.90)

Table A.2. Probability ratio and change in intensity of an event such as the recent 2023/24 August-July temperature due to changing GMST, for Sardinia: (a) from pre industrial climate to the present and (b) from the present to 2C above preindustrial.

	a. Past vs. present		**b. Present vs. future**	
Model / Observations	**Probability ratio PR [-]**	**Change in intensity ΔI [units]**	**Probability ratio PR [-]**	**Change in intensity ΔI [units]**

ERA5	3.2e+10 (9.0e+7 ... 3205916286802642)	2.1 (1.7 ... 2.5)		
MSWEP	19466246961204724 (8.8e+10 ... 2.3e+27)	2.9 (2.2 ... 3.5)		
CPC	7.6e+20 (4.9e+13 ... 1.9e+36)	2.9 (2.2 ... 3.5)		
CNRM-CM5_CCLM4-8-17 ()	1.6e+2 (8.9 ... 9.2e+3)	0.86 (0.42 ... 1.3)	9.5 (6.6 ... 15)	0.64 (0.52 ... 0.77)
CNRM-CM5_COSMO-crCLIM-v1-1 ()	3.0e+2 (14 ... 2.2e+4)	0.88 (0.46 ... 1.3)	7.6 (5.3 ... 11)	0.48 (0.39 ... 0.58)
CNRM-CM5_KNMI-RACMO22E ()	7.6e+2 (34 ... 1.0e+5)	1.0 (0.62 ... 1.5)	10 (7.3 ... 16)	0.63 (0.53 ... 0.74)
EC-EARTH_COSMO-crCLIM-v1-1 ()	1.1e+7 (1.4e+5 ... 1.9e+10)	2.0 (1.7 ... 2.4)	12 (8.1 ... 19)	0.77 (0.64 ... 0.90)
EC-EARTH_RACMO22E ()	3.0e+8 (1.8e+6 ... 3.9e+12)	1.9 (1.6 ... 2.2)	17 (12 ... 26)	0.81 (0.69 ... 0.91)
HadGEM2-ES_COSMO-crCLIM-v1-1 ()	3.2e+3 (1.7e+2 ... 5.4e+5)	1.6 (1.1 ... 2.0)	9.5 (7.2 ... 13)	0.78 (0.68 ... 0.88)
HadGEM2-ES_RegCM4-6 ()	4.3e+6 (9.5e+4 ... 2.1e+10)	1.6 (1.3 ... 2.0)	21 (16 ... 29)	0.82 (0.74 ... 0.91)
MPI-ESM-LR_CCLM4-8-17 ()	2.8e+3 (2.0e+2 ... 1.3e+5)	1.3 (0.95 ... 1.7)	9.9 (7.2 ... 14)	0.73 (0.61 ... 0.85)
MPI-ESM-LR_COSMO-crCLIM-v1-1 ()	4.0e+2 (45 ... 1.1e+4)	1.1 (0.78 ... 1.5)	8.0 (5.9 ... 11)	0.65 (0.53 ... 0.76)
MPI-ESM-LR_RegCM4-6 ()	1.1e+4 (2.5e+2 ... 7.0e+6)	1.1 (0.75 ... 1.6)	15 (11 ... 22)	0.69 (0.57 ... 0.81)
MPI-ESM-LR_RACMO22E ()	8.4e+2 (75 ... 3.4e+4)	1.1 (0.80 ... 1.5)	9.0 (6.5 ... 13)	0.64 (0.53 ... 0.74)
MPI-ESM-LR_REMO2009 ()	3.6e+3 (2.5e+2 ... 1.8e+5)	1.3 (0.98 ... 1.6)	11 (7.6 ... 16)	0.73 (0.62 ... 0.83)
MPI-ESM-LR_WRF361H ()	4.1e+8 (14 ... 7.7e+31)	2.4 (0.36 ... 4.3)	15 (7.3 ... 27)	0.78 (0.48 ... 1.1)
NorESM1-M_-REMO2015 ()	3.5e+7 (3.4e+5 ... 5.4e+10)	1.8 (1.5 ... 2.1)	20 (14 ... 28)	0.91 (0.79 ... 1.0)
NorESM1-M_RegCM4-6 ()	4.1e+9 (9.0e+6 ... 7.6e+14)	1.7 (1.3 ... 2.1)	27 (21 ... 37)	0.83 (0.73 ... 0.94)

Table A.3. Probability ratio and change in intensity of an event such as the recent 2023/24 August-July low precipitation due to changing GMST, for Sicily: (a) from pre industrial climate to the present and (b) from the present to 2C above preindustrial.

	a. Past vs. present		**b. Present vs. future**	
Model / Observations	**Probability ratio PR [-]**	**Change in intensity ΔI [units]**	**Probability ratio PR [-]**	**Change in intensity ΔI [units]**

ERA5	3.1 (1.1 ... 12)	-13 (-24 ... -1.0)		
ERA5-precal	1.0 (0.22 ... 8.0)	-0.0097 (-22 ... 26)		
MSWEP	0.39 (0.054 ... 1.9)	14 (-7.9 ... 51)		
CNRM-CM5_CCLM4-8-17 ()	1.45 (0.56..5.40)	-7.9(-24.83..15.4)	1.13(0.90.. 1.53)	-3.31 (-10.73..2.52)
CNRM-CM5_COSMO-crCLIM-v1-1 ()	1.13 (0.45..2.86)	-2.56 (-18.82.. 17.12)	1.018(0.77..1.48)	-0.472 (-9.24..6.14)
CNRM-CM5_KNMI-RACMO22E ()	0.69 (0.20..2.19)	6.07 -11.17.. 29.0)	0.89 (4 0.66.. 1.20)	2.31 (-3.25..8.15)
EC-EARTH_COSMO-crCLIM-v1-1 ()	1.28 (0.78..2.24)	-10.0 (-28.27.. 8.3)	1.2 (1.0.. 1.44)	-6.10 (-12.83..-0.005)
EC-EARTH_RACMO22E ()	0.70 (2 0.20… 2.19)	0.012 (-17.53.. 15.52)	0.93 (0.69.. 1.18)	1.42 (-3.95..6.40)
HadGEM2-ES_CCLM4-8-17 ()	1.08 (5 0.52.. 3.06)	-1.9 (-20.68.. 15.09)	0.93 (0.79.. 1.09)	2.08 (-2.42..16.22)
HadGEM2-ES_COSMO-crCLIM-v1-1 ()	1.57 (0.84.. 4.73)	-13 (-31.88..5.53)	0.91 (0.78.. 1.09)	3.00(-2.52.. 7.90)
HadGEM2-ES_RegCM4-6 ()	0.87 (0.39.. 2.05)		1.03 (0.70.. 1.63)	
HadGEM2-ES_RACMO22E ()	0.87 (0.39.. 2.05)	2.32 (-11.33..15.5)	0.93 (0.74.. 1.20)	1.34 (-3.00..6.17)
MPI-ESM-LR_CCLM4-8-17 ()	0.78 (0.3.. 2.03)	4.6 (-10.74..24.32)	1.13 (0.91.. 1.44)	-2.78 (-8.373..2.12)
MPI-ESM-LR_COSMO-crCLIM-v1-1 ()	0.99 (0.42.. 2.1)	0.3 (-14.09..23.15)	1.11 (0.92.. 1.47)	-3.75 (-10.64..3.27)
MPI-ESM-LR_RegCM4-6 ()	0.91 (0.21.. 3.67)	1.09 (-11.8..18.23)	1.56(1.07.. 2.4)	-5.52 (-10.59.. -0.84)
MPI-ESM-LR_RACMO22E ()	0.63 (0.26.. 1.45)	8.19(-5.45..26.40)	1.14 (0.89.. 1.52)	-2.61 (-7.28..2.5)
MPI-ESM-LR_REMO2009 ()	1.09 (0.49.. 2.4)	-2.6 (-18.87..21.00)	1.25 (1.036..1.66)	-7.97 (-14.9..-1.49)
MPI-ESM-LR_WRF361H ()	8.23 (2.34..53)	-37.97 (-77.58.. -14.14)	1.79 (0.94.. 4.59)	-14.96 (-37.00..1.23)
NorESM1-M_-REMO2015 ()	1.29 (0.37.. 4.81)	-3.67 (-19.36.. 14.55)	1.00 (0.71.. 1.4)	-0.01(.. -4.85.. 4.68)

Table A.4. Probability ratio and change in intensity of an event such as the recent 2023/24 August-July temperature due to changing GMST, for Sicily: (a) from pre industrial climate to the present and (b) from the present to 2C above preindustrial.

	a. Past vs. present	**b. Present vs. future**
Model / Observations		

	Probability ratio PR [-]	Change in intensity ΔI [units]	Probability ratio PR [-]	Change in intensity ΔI [units]
ERA5	5.1e+8 (2.1e+6 ... 1.2e+13)	1.7 (1.3 ... 2.1)		
MSWEP	5.5e+14 (4.1e+9 ... 1.8e+27)	2.5 (1.9 ... 3.2)		
CPC	2.2e+3 (4.6 ... 1.4e+7)	0.98 (0.19 ... 1.7)		
CNRM-CM5_CCLM4-8-17 ()	3.0e+3 (94 ... 4.6e+5)	1.1 (0.71 ... 1.5)	18 (12 ... 29)	0.73 (0.62 ... 0.85)
CNRM-CM5_COSMO-crCLIM-v1-1 ()	9.6e+2 (26 ... 1.4e+5)	0.89 (0.49 ... 1.3)	14 (8.7 ... 23)	0.56 (0.46 ... 0.64)
CNRM-CM5_KNMI-RACMO22E ()	1.7e+5 (2.8e+3 ... 1.6e+8)	1.3 (0.98 ... 1.7)	29 (20 ... 44)	0.77 (0.68 ... 0.87)
EC-EARTH_COSMO-crCLIM-v1-1 ()	1.3e+8 (9.5e+5 ... 1.4e+12)	1.9 (1.6 ... 2.2)	26 (18 ... 39)	0.79 (0.70 ... 0.88)
EC-EARTH_RACMO22E ()	2.7e+8 (1.4e+6 ... 2.6e+12)	1.8 (1.6 ... 2.2)	28 (20 ... 42)	0.80 (0.70 ... 0.89)
HadGEM2-ES_CCLM4-8-17 ()	1.1e+7 (2.3e+5 ... 7.4e+9)	1.8 (1.5 ... 2.1)	27 (20 ... 39)	0.85 (0.77 ... 0.93)
HadGEM2-ES_COSMO-crCLIM-v1-1 ()	6.4e+5 (1.3e+4 ... 5.1e+8)	1.8 (1.4 ... 2.1)	19 (14 ... 28)	0.79 (0.71 ... 0.87)
HadGEM2-ES_RACMO22E ()	1.3e+6 (2.8e+4 ... 1.4e+9)	1.8 (1.4 ... 2.1)	23 (17 ... 33)	0.82 (0.74 ... 0.90)
MPI-ESM-LR_CCLM4-8-17 ()	2.3e+4 (1.3e+3 ... 1.7e+6)	1.4 (1.0 ... 1.7)	17 (12 ... 25)	0.73 (0.63 ... 0.83)
MPI-ESM-LR_COSMO-crCLIM-v1-1 ()	4.7e+3 (3.7e+2 ... 3.8e+5)	1.2 (0.89 ... 1.5)	14 (9.8 ... 22)	0.69 (0.57 ... 0.80)
MPI-ESM-LR_RegCM4-6 ()	8.3e+4 (6.0e+2 ... 8.0e+8)	1.2 (0.77 ... 1.7)	24 (16 ... 40)	0.70 (0.58 ... 0.83)
MPI-ESM-LR_RACMO22E ()	4.7e+3 (2.6e+2 ... 4.3e+5)	1.2 (0.87 ... 1.5)	14 (9.1 ... 22)	0.67 (0.56 ... 0.77)
MPI-ESM-LR_REMO2009 ()	9.3e+4 (3.6e+3 ... 1.6e+7)	1.4 (1.1 ... 1.7)	21 (14 ... 33)	0.79 (0.68 ... 0.89)
MPI-ESM-LR_WRF361H ()	3.6e+14 (2.0e+4 ... 1.2e+50)	2.5 (0.98 ... 3.8)	30 (14 ... 56)	0.82 (0.56 ... 1.1)
NorESM1-M_COSMO-crCLIM-v1-1 ()	3.4e+7 (9.8e+4 ... 1.7e+11)	1.4 (1.1 ... 1.7)	35 (26 ... 52)	0.80 (0.71 ... 0.90)
NorESM1-M_RegCM4-6 ()	7.5e+11 (4.3e+8 ... 4204487417636692480)	1.7 (1.4 ... 2.1)	52 (38 ... 72)	0.83 (0.74 ... 0.94)

(a) Probabilty ratio (past to present)

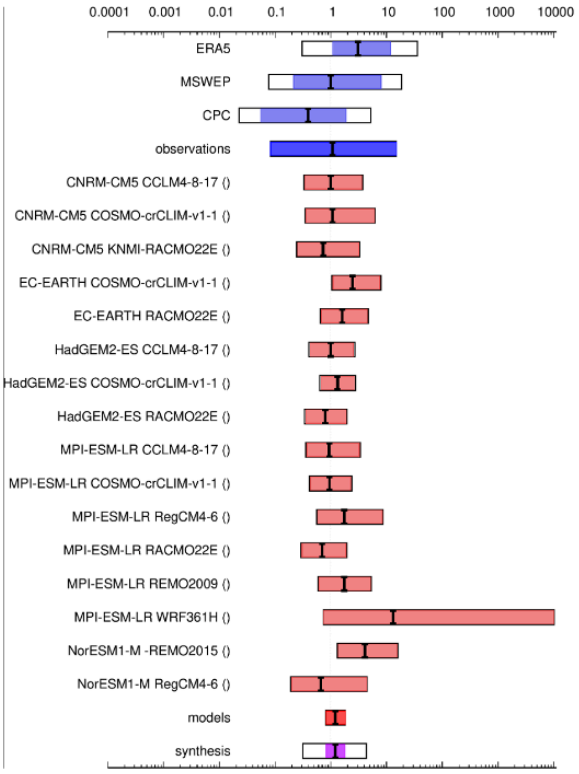

(b) Intensity change (past to present)

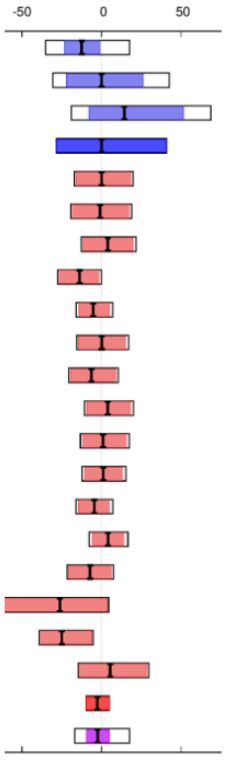

(c) Probabilty ratio (present to future)

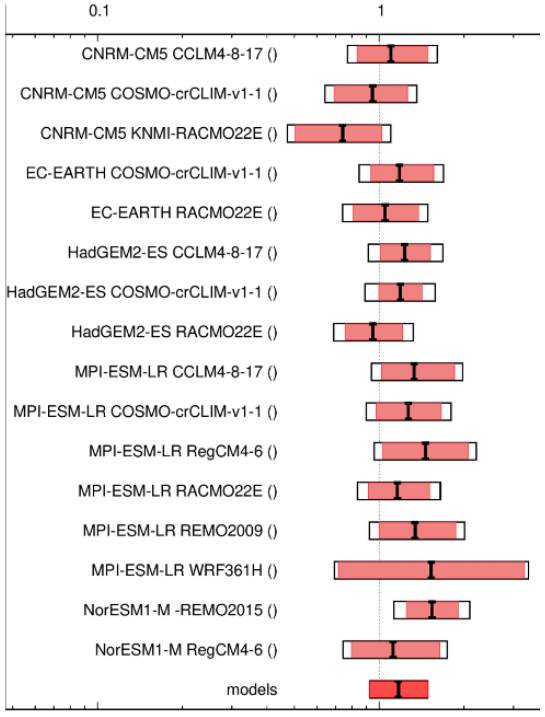

(d) Intensity change (present to future)

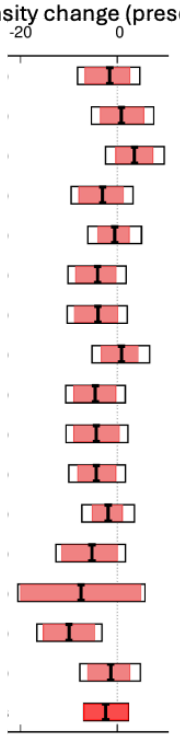

Fig. A1 (a left) Synthesis of probability ratios and (b right) intensity changes in annual (Aug-July) cumulative precipitation, when comparing the return period and magnitudes of the 2023/24 Aug-July cumulative precipiation over Sardinia in the current climate and a 1.3°C cooler climate. (c left) same as (a) in the current climate and a 0.7°C cooler climate. (d right) same as (b) in the current climate and a 0.7°C cooler climate.

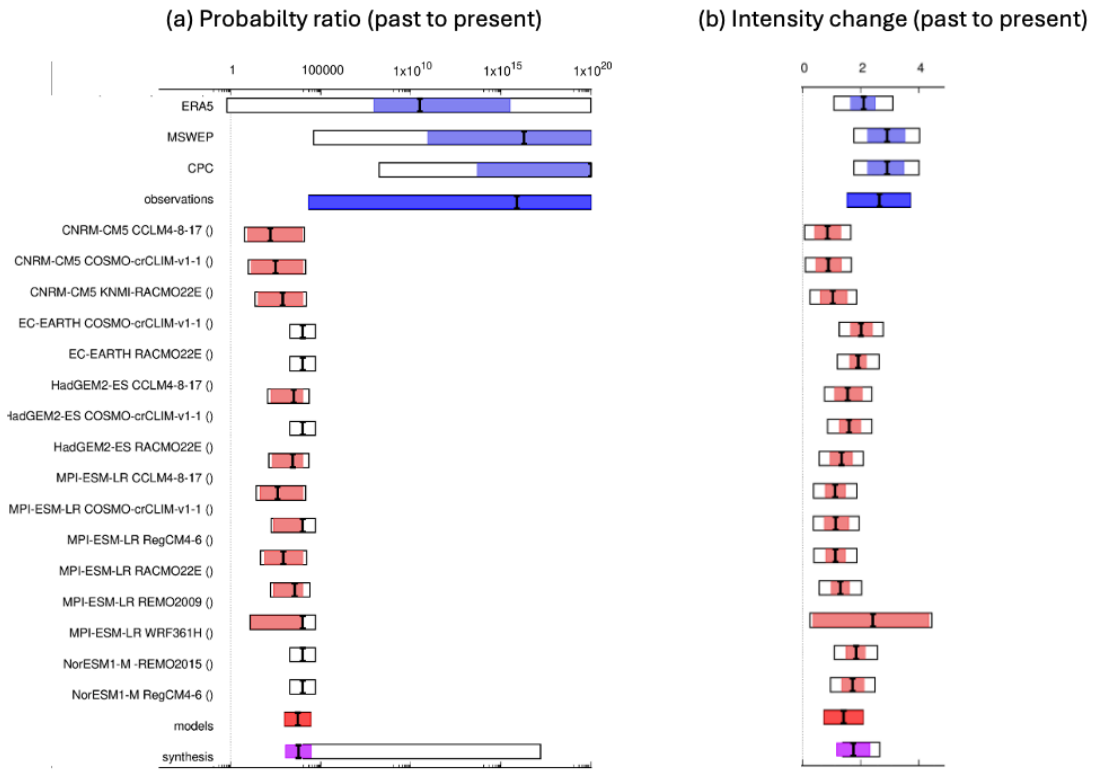

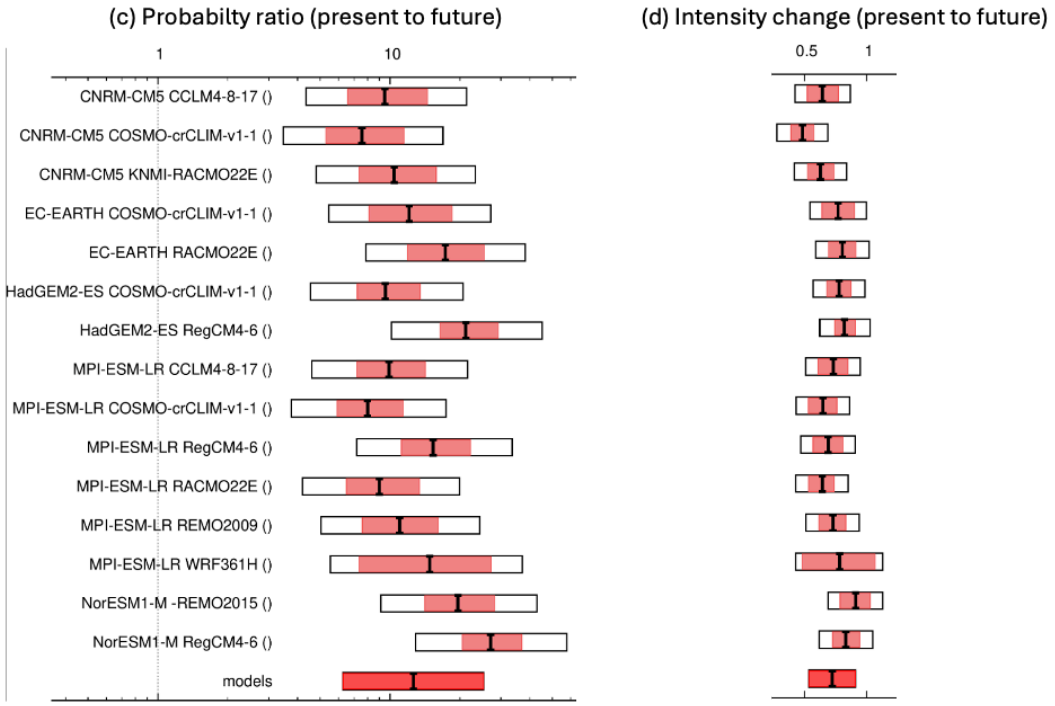

Fig. A2 (a left) Synthesis of probability ratios and (b right) intensity changes in annual (Aug-July) temperature, when comparing the return period and magnitudes of the 2023/24 Aug-July average temperature over Sardinia in the current climate and a 1.3°C cooler climate. (c left) same as (a) in the current climate and a 0.7°C cooler climate. (d right) same as (b) in the current climate and a 0.7°C cooler climate.

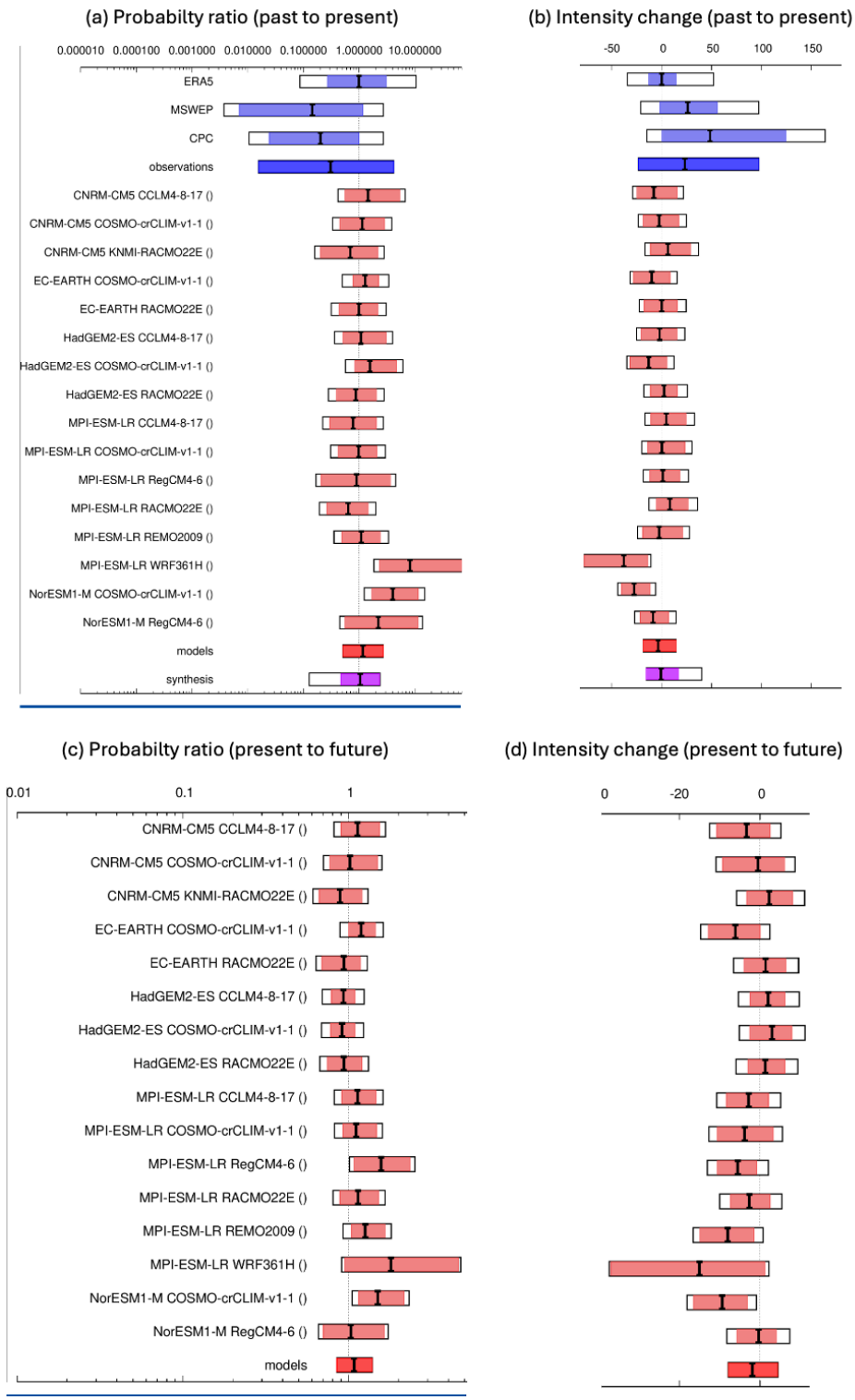

Fig. A3 (a left) Synthesis of probability ratios and (b right) intensity changes in annual (Aug-July) cumulative precipitation, when comparing the return period and magnitudes of the 2023/24 Aug-July cumulative precipiation over Sicily in the current climate and a 1.3°C cooler climate. (c left) same as (a) in the current climate and a 0.7°C cooler climate. (d right) same as (b) in the current climate and a 0.7°C cooler climate.

(a) Probabilty ratio (past to present)

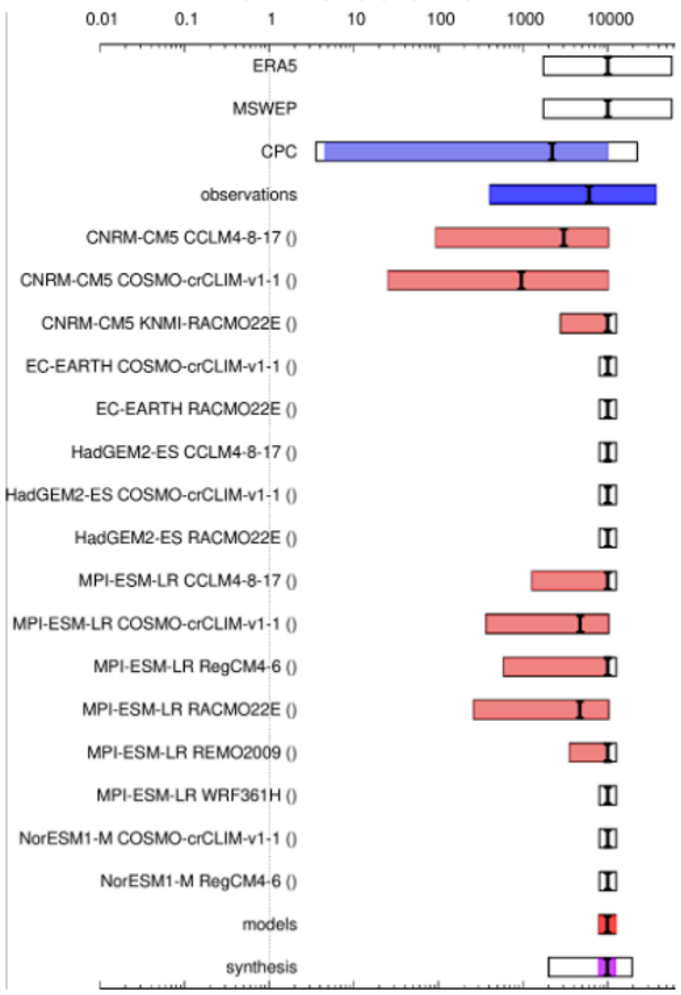

(b) Intensity change (past to present)

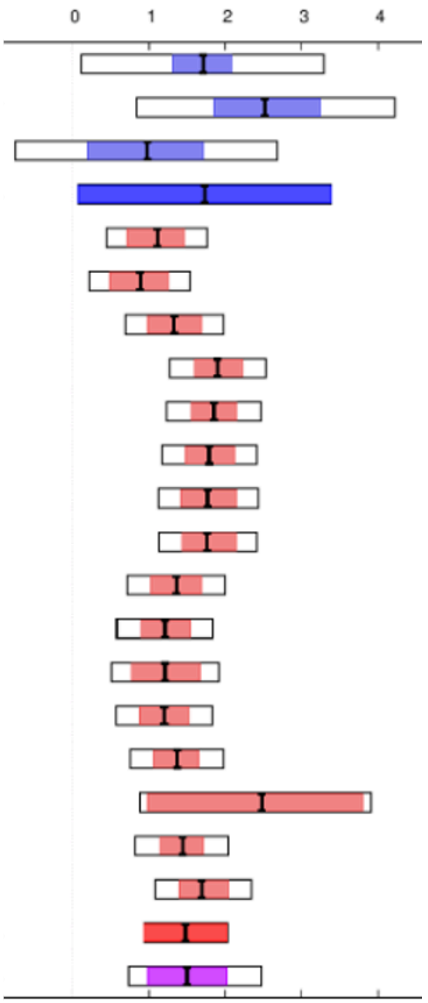

(c) Probabilty ratio (present to future)

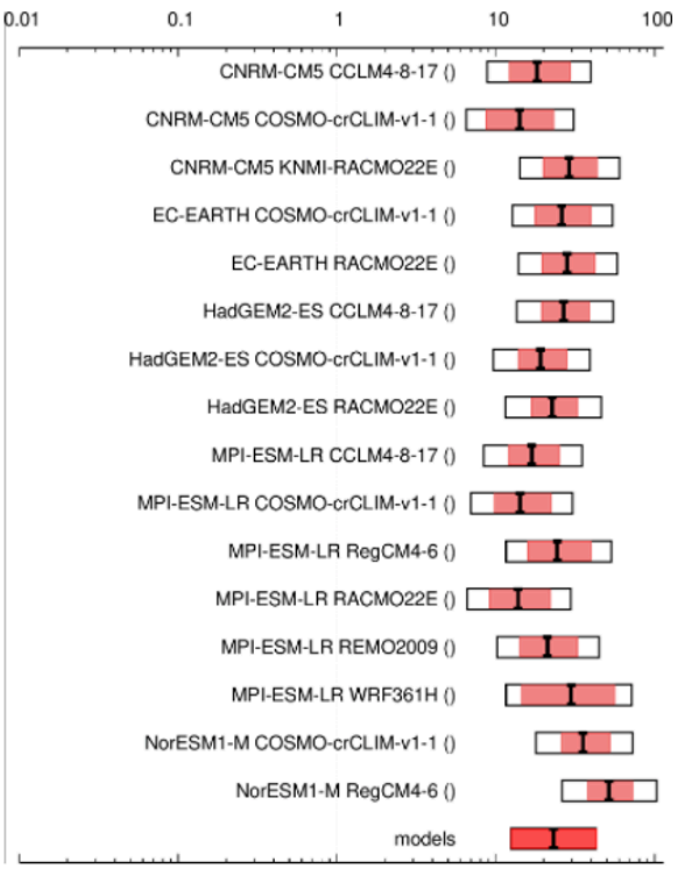

(d) Intensity change (present to future)

Fig. A4 (a left) Synthesis of probability ratios and (b right) intensity changes in annual (Aug-July) temperature, when comparing the return period and magnitudes of the 2023/24 Aug-July average temperature over Sicily in the current climate and a 1.3°C cooler climate. (c left) same as (a) in the current climate and a 0.7°C cooler climate. (d right) same as (b) in the current climate and a 0.7°C cooler climate.

References

All references are given as hyperlinks in the text.